

Unadjusted Hamiltonian MCMC with Stratified Monte Carlo Time Integration

Nawaf Bou-Rabee¹ and Milo Marsden²

¹*Department of Mathematical Sciences
Rutgers University Camden
311 N 5th Street
Camden, NJ 08102 USA
nawaf.bourabee@rutgers.edu*

²*Department of Mathematics
Stanford University
450 Jane Stanford Way
Stanford, CA 94025 USA
mmarsden@stanford.edu*

Abstract: A novel randomized time integrator is suggested for unadjusted Hamiltonian Monte Carlo (uHMC) in place of the usual Verlet integrator; namely, a stratified Monte Carlo (sMC) integrator which involves a minor modification to Verlet, and hence, is easy to implement. For target distributions of the form $\mu(dx) \propto e^{-U(x)}dx$ where $U : \mathbb{R}^d \rightarrow \mathbb{R}_{\geq 0}$ is both K -strongly convex and L -gradient Lipschitz, and initial distributions ν with finite second moment, coupling proofs reveal that an ε -accurate approximation of the target distribution μ in L^2 -Wasserstein distance \mathcal{W}^2 can be achieved by the uHMC algorithm with sMC time integration using $O((d/K)^{1/3}(L/K)^{5/3}\varepsilon^{-2/3} \log(\mathcal{W}^2(\mu, \nu)/\varepsilon)^+)$ gradient evaluations; whereas without additional assumptions the corresponding complexity of the uHMC algorithm with Verlet time integration is in general $O((d/K)^{1/2}(L/K)^2\varepsilon^{-1} \log(\mathcal{W}^2(\mu, \nu)/\varepsilon)^+)$. Duration randomization, which has a similar effect as partial momentum refreshment, is also treated. In this case, without additional assumptions on the target distribution, the complexity of duration-randomized uHMC with sMC time integration improves to $O(\max((d/K)^{1/4}(L/K)^{3/2}\varepsilon^{-1/2}, (d/K)^{1/3}(L/K)^{4/3}\varepsilon^{-2/3}))$ up to logarithmic factors. The improvement due to duration randomization turns out to be analogous to that of time integrator randomization.

MSC 2010 subject classifications: Primary 60J05; secondary 65C05, 65P10.

Keywords and phrases: MCMC, Hamiltonian Monte Carlo, Couplings.

1. Introduction

Consider a ‘target’ probability distribution of the form $\mu(dx) \propto e^{-U(x)}dx$ where $U : \mathbb{R}^d \rightarrow \mathbb{R}_{\geq 0}$ is continuously differentiable. Hamiltonian Monte Carlo (HMC) is an MCMC method aimed at μ that incorporates a measure-preserving Hamiltonian dynamics per transition step [18, 36]. The dynamics are typically discretized using a *deterministic* time integrator, and the discretization bias can either be borne (*unadjusted* HMC or *uHMC* for short) or eliminated by a Metropolis-Hastings filter (*adjusted* HMC). In this work, a new time integrator is suggested for Hamiltonian MCMC, one that is better suited for the probabilistic aims of

MCMC. The basic idea is to use a simple, randomized method to time discretize the Hamiltonian dynamics. This strategy turns out to improve upon the current state of the art for uHMC.

Throughout this work, we focus on K -strongly convex and L -gradient Lipschitz U , and state complexity guarantees in terms of the L^2 -Wasserstein distance \mathcal{W}^2 . The strong convexity assumption on U can be relaxed to, e.g., asymptotic strong convexity — as in [6, 15, 8]. However, the resulting contraction rates, and in turn, asymptotic bias and complexity estimates will then depend on model and hyperparameters in a more involved way. On the other hand, the dependence on model and hyperparameters is more clear under global strong convexity, and therefore, the strongly convex setting allows for more precise mathematical comparisons between algorithms. Consequently, as we review below, the strongly convex setting has been the focus of much of the existing literature [12, 29, 35, 39].

1.1. State of the Art.

At present, the Verlet time integrator is the method of choice for time integrating the Hamiltonian dynamics in both unadjusted and adjusted HMC [4]. This is not without reason. Indeed, the Verlet integrator is cheap; like forward Euler it requires only one new gradient evaluation per integration step. At the same time, the Verlet integrator is also second-order accurate under sufficiently strong regularity assumptions — more on this point below. Remarkably, the Verlet integrator also has the maximal stability interval for the simple harmonic model problem [2, 11]. These properties are quite relevant to uHMC [8]. Moreover, the geometric properties of the Verlet integrator (symplecticity and reversibility) are key to obtaining an evaluable Metropolis-Hastings ratio in adjusted HMC [21, 4]. Not surprisingly, most of the research work on HMC has been devoted to the study of unadjusted and adjusted HMC with Verlet time integration.

A notable exception is the work of Lee, Song and Vempala [29]. In that work, the authors suggest to use uHMC with a collocation method for the Hamiltonian dynamics to resolve the asymptotic bias. This collocation method relies on a choice of basis functions (usually polynomials up to a certain degree) to represent the exact solution, and uses a nonlinear solver per uHMC transition step. General complexity guarantees are given for their ODE solvers, and as an application of their ideas to Hamiltonian MCMC, they consider the special case of a basis of piecewise quadratic polynomials defined on a time grid of step size h . In this case, uHMC with collocation can in principle produce an ε -accurate approximation of the target μ in \mathcal{W}^2 distance using

$$O\left(\left(\frac{d}{K}\right)^{1/2} \left(\frac{L}{K}\right)^{1.75} \varepsilon^{-1} \log\left(\frac{d}{K^{1/2}} \frac{L}{K} \frac{1}{\varepsilon}\right)^+ \log\left(\frac{d}{K^{1/2}\varepsilon}\right)^+\right) \text{ gradient evaluations} \quad (1)$$

when initialized at the minimum of U and run with duration $T \propto K^{1/4}/L^{3/4}$. In each transition step of uHMC, h is chosen to satisfy $h^{-1} \propto LT^3(|v| + |\nabla U(x)|T)K^{1/2}(L/K)^{3/2}\varepsilon^{-1}$, where $x, v \in \mathbb{R}^d$ are respectively the initial position and velocity in the current transition step. See [29, Theorem 1.6] for a

detailed statement. Remarkably, the dimension dependence is $d^{1/2}$ and the condition number dependence is $(L/K)^{1.75}$. Moreover, this complexity guarantee requires no regularity beyond L -gradient Lipschitz-ness and K -strong convexity of U . In practice, because uHMC with collocation requires a nonlinear solve per transition step, its widespread use is limited.

For comparison, in the absence of any higher regularity, the corresponding complexity for uHMC with Verlet time integration is

$$O\left(\left(\frac{d}{K}\right)\left(\frac{L}{K}\right)^2 \varepsilon^{-1} \log\left(\frac{\mathcal{W}^2(\mu, \nu)}{\varepsilon}\right)^+\right) \text{ gradient evaluations} \quad (2)$$

when initialized from a distribution ν with finite second moment and run with time step size $h \propto (L/K)^{-3/2} d^{-1/2} \varepsilon$ and duration $T \propto L^{-1/2}$. See [3, Chapter 5] for detailed statements and proofs of (2); which is based on [8, Appendix A].

Note that uHMC with Verlet substantially underperforms uHMC with collocation in terms of dimension and condition number dependence. This substandard performance is because the theoretical second order accuracy of Verlet integration typically requires U to be thrice differentiable with bounded third derivative [5, Lemma 23]. Indeed, under only the assumption that U is L -gradient Lipschitz, the order of accuracy of Verlet integration often drops to first order [8, Theorem 3.6]. This drop in accuracy is ultimately due to the fact that Verlet uses a trapezoidal approximation of the integral of the force $-\nabla U$, and it is well known that the trapezoidal rule typically drops an order of accuracy if the integrand does not have a bounded second derivative. In turn, the accuracy of the integration scheme affects the asymptotic bias between the invariant measure of uHMC and the target distribution. Thus, a smaller time step size is needed to resolve the asymptotic bias of uHMC, which in turn requires more gradient evaluations.

In principle, adjusted HMC can filter out all of the asymptotic bias due to time discretization. One would therefore hope that the dependence of the complexity on the accuracy parameter ε becomes logarithmic with adjustment. This result has recently been demonstrated under higher regularity conditions and some restrictions on the initial conditions; specifically, assuming U is strongly convex, gradient Lipschitz and Hessian Lipschitz, Chen, Dwivedi, Wainwright, and Yu use a clever conductance argument to prove that adjusted HMC with Verlet from a ‘warm’ start can achieve ε accuracy in total variation distance using $O(d^{11/12}(L/K) \log(1/\varepsilon)^+)$ gradient evaluations [12]. In the same setting, implementable starting distributions are also considered; specifically, from a ‘feasible’ start, the complexity becomes $O(\max(d(L/K)^{3/4}, d^{11/12}(L/K), d^{3/4}(L/K)^{5/4}, d^{1/2}(L/K)^{3/2})) \log(1/\varepsilon)^+)$ gradient evaluations to reach ε accuracy. In both complexity estimates, note the remarkable logarithmic dependence on ε . At present, it remains an open problem to relax the Hessian Lipschitz regularity assumption and the warm/feasible start conditions.

In very recent work, Monmarché considers a parameterized family of algorithms which include as special cases uHMC with Verlet time integration and a

class of time discretizations for Underdamped Langevin Diffusions (ULD) [35]. For Gaussian target measures, the optimal algorithms within this family are remarkably ULD based algorithms and uHMC with partial velocity refreshment. In the strongly convex and gradient Lipschitz case, and for a wide range of parameters, dimension free lower bounds on the convergence rate of the corresponding algorithms are provided. Specializing to the case where U is additionally Hessian Lipschitz, unified complexity guarantees are given for suitably tuned versions of both ULD based and uHMC-like algorithms within the class under consideration. In particular, focussing only on the dependence in dimension d and accuracy ε , an ε -accurate approximation of the target distribution μ can be achieved by these algorithms in $O(d^{1/2}\varepsilon^{-1/2}\log(d/\varepsilon))$ gradient evaluations. Moreover, when the condition number is large, Monmarché notes the superiority of partial momentum refreshment over complete refreshment. In particular, in the Gaussian setting, an improved contraction rate for uHMC with partial momentum refreshment is observed, i.e., from K/L to $(K/L)^{1/2}$ — more on this point below.

Our work is strongly inspired by the recent success of the Randomized Mid-point Method (RMM) due to Shen and Lee [39]. The RMM method is obtained by using a randomized time integrator applied to ULD. Synchronously coupling RMM with exact ULD, Shen and Lee prove that RMM can produce an ε -accurate approximation of the target in \mathcal{W}^2 distance using

$$O\left(\left(\frac{d}{K}\right)^{1/6}\left(\frac{L}{K}\right)^{7/6}\varepsilon^{-1/3}\left(\log\left(\frac{d^{1/2}}{K^{1/2}\varepsilon}\right)^+\right)^{7/6} + \left(\frac{d}{K}\right)^{1/3}\left(\frac{L}{K}\right)\varepsilon^{-2/3}\left(\log\left(\frac{d^{1/2}}{K^{1/2}\varepsilon}\right)^+\right)^{4/3}\right) \quad (3)$$

gradient evaluations when initialized at rest within $(d/K)^{1/2}$ of the minimum of U and run with time step size satisfying

$$h \propto \min\left(\frac{K^{1/3}}{d^{1/6}L^{1/6}}\varepsilon^{1/3}\left(\log\left(\frac{d^{1/2}}{K^{1/2}\varepsilon}\right)^+\right)^{1/6}, \frac{K^{1/3}}{d^{1/3}}\varepsilon^{2/3}\left(\log\left(\frac{d^{1/2}}{K^{1/2}\varepsilon}\right)^+\right)^{1/3}\right),$$

friction 2, and mass L . The proof uses a perturbative approach that leverages the contractivity of exact ULD [14, 16] to bound the \mathcal{W}^2 distance between the distribution of the corresponding RMM chain and the target distribution. Ergodicity of the RMM chain and a $3/2$ -order of accuracy for the \mathcal{W}^2 -asymptotic bias of RMM was subsequently proven in [23].

Additionally, Cao, Lu, and Wang demonstrate the optimality of RMM among a class of ULD based sampling algorithms [10]. Specifically, the authors show that any randomized algorithm for simulating ULD which makes N combined queries to ∇U , the driving Brownian motion, and the weighted integral of Brownian motion will suffer worst case L^2 -error of order at least $\Omega(d^{1/2}N^{-3/2})$. Thus, to guarantee an ε -accurate approximation of ULD in \mathcal{W}^2 distance, one requires N to be at least $\Omega(d^{1/3}\varepsilon^{-2/3})$ — matching the upper bound on the L^2 -error for RMM in dimension d and accuracy ε . Ref. [10] also contains many references to the existing literature on information theoretic lower bounds for randomized simulation of ODEs and SDEs, such as [27], [26], [17].

Another related work is the shifted ODE method for ULD due to Foster, Lyons and Oberhauser [22]. In the gradient Lipschitz and strongly convex case, the shifted ODE method produces in principle an ε -accurate approximation of the target distribution in \mathfrak{W}^2 distance using $O(d^{1/3}\varepsilon^{-2/3})$ gradient evaluations with even better complexity guarantees under stronger smoothness assumptions. The shifted ODE method is inspired by rough path theory, in which SDEs are realized as instances of Controlled Differential Equations (CDE). In particular, the shifted ODE method is constructed by tuning a controlling path such that the Taylor expansion of the CDE solution has the same low order terms as ULD. In practice, the ODE they obtain cannot be time integrated exactly, so they propose two implementable methods based on a third order Runge-Kutta method and a fourth order splitting method. Numerical results for the discretizations are promising. The challenge is that the discretizations are trickier to analyze than the exact shifted ODE method.

In view of the complexity guarantees (1), (2), and (3), it is natural to ask: *Is it possible to construct a randomized time integrator for unadjusted Hamiltonian MCMC that does not require a nonlinear solver or higher regularity of U and that confers a better complexity guarantee for the corresponding uHMC algorithm?* Since Hamiltonian dynamics does not explicitly incorporate friction or diffusion like ULD does [32, 7], it is not at all obvious that uHMC with an RMM-type method would have a provably better complexity guarantee than uHMC with Verlet. At a technical level, understanding the contractivity and asymptotic bias of the corresponding uHMC algorithm requires developing new mathematical arguments to quantify the effects of randomization in the approximation of the Hamiltonian dynamics. This paper answers the above question in the affirmative by suggesting a simple stratified Monte Carlo time integrator for Hamiltonian MCMC and carefully analyzing the properties of the corresponding uHMC algorithm. To be sure, while Monte Carlo methods are generally intended for high-dimensional integration, stratified Monte Carlo methods are actually better suited for one-dimensional integration, such as time integration.

1.2. Short Overview of Main Results.

We now outline our main contributions. As above, we consider a target distribution $\mu(dx) \propto e^{-U(x)}dx$ where $U : \mathbb{R}^d \rightarrow \mathbb{R}_{\geq 0}$ is continuously differentiable, K -strongly convex and L -gradient Lipschitz. Let $(q_t(x, v), v_t(x, v))$ denote the exact flow of the Hamiltonian dynamics

$$\frac{d}{dt}q_t = v_t, \quad \frac{d}{dt}v_t = -\nabla U(q_t), \quad (q_0, v_0) = (x, v).$$

In this context, we introduce the stratified Monte Carlo (sMC) time integrator. Let $h > 0$ be a time step size and $\{t_k := kh\}_{k \in \mathbb{N}_0}$ be an evenly spaced time grid. This grid partitions time into subintervals $\{[t_k, t_{k+1})\}_{k \in \mathbb{N}_0}$ termed ‘strata’. One step of the sMC time integrator from t_i to t_{i+1} is given by

$$\tilde{Q}_{t_{i+1}} = \tilde{Q}_{t_i} + h\tilde{V}_{t_i} + \frac{1}{2}h^2\tilde{F}_{t_i}, \quad \tilde{V}_{t_{i+1}} = \tilde{V}_{t_i} + h\tilde{F}_{t_i}, \quad (\tilde{Q}_0, \tilde{V}_0) = (x, v), \quad (4)$$

where $\tilde{F}_{t_i} = -\nabla U(\tilde{Q}_{t_i} + (\mathcal{U}_i - t_i)\tilde{V}_{t_i})$ and $(\mathcal{U}_i)_{i \in \mathbb{N}_0}$ is a sequence of independent random variables such that $\mathcal{U}_i \sim \text{Uniform}(t_i, t_{i+1})$. In words, \mathcal{U}_i is a random temporal sample point sampled uniformly from the i -th stratum, and independent of the sample points in the other strata. Note that the sMC time integrator is *explicit* in the sense that $(\tilde{Q}_{t_{i+1}}, \tilde{V}_{t_{i+1}})$ is an explicit function of $(\tilde{Q}_{t_i}, \tilde{V}_{t_i})$.

One intuition behind this scheme is as follows. Like Verlet integration, the sMC integrator updates the position variable on the i -th stratum $[t_i, t_{i+1})$ by a constant force \tilde{F}_{t_i} . However, unlike Verlet integration, the update rule involves the force evaluated at a random temporal sample point \mathcal{U}_i sampled from the i -th stratum, rather than always the left temporal endpoint t_i . Moreover, unlike Verlet integration, the sMC integrator updates the velocity variable on the i -th stratum $[t_i, t_{i+1})$ by the same constant force \tilde{F}_{t_i} . Thus, this scheme uses only one new gradient evaluation per sMC integration step. This scheme is probably the simplest randomized time integrator for the Hamiltonian dynamics, but it certainly is not the only strategy. For example, one could approximate the force over the i -th stratum as $-\nabla U(q_{\mathcal{U}_i}(\tilde{Q}_{t_i}, \tilde{V}_{t_i}))$. However, as the true dynamics are unknown, this is not implementable. Choosing instead to first approximate $q_{\mathcal{U}_i}(\tilde{Q}_{t_i}, \tilde{V}_{t_i})$ using the forward Euler method, and then using the force at the resulting (random) point to approximate the dynamics for both position and velocity over the i -th stratum $[t_i, t_{i+1})$ results in the sMC method described above. Replacing Verlet integration in this way, we obtain the uHMC algorithm with complete momentum refreshment described in Algorithm 1.

Algorithm 1: uHMC Transition Step with sMC Time Integration

Input: Current state of the chain $X_0 \in \mathbb{R}^d$, duration $T > 0$ and time step size $h > 0$.

- 1 Sample ξ from $\mathcal{N}(0, I_d)$;
- 2 Initialize sMC time integrator $\tilde{Q}_0 = X_0$; $\tilde{V}_0 = \xi$; $t_0 = 0$; $n = \lceil T/h \rceil$;
- 3 **for** $i = 0$ **to** $i = n - 1$ **do**
- 4 Update time $t_{i+1} = t_i + h$;
- 5 Sample \mathcal{U}_i uniformly from (t_i, t_{i+1}) ;
- 6 Evaluate potential force $\tilde{F}_{t_i} = -\nabla U(\tilde{Q}_{t_i} + (\mathcal{U}_i - t_i)\tilde{V}_{t_i})$;
- 7 Update position $\tilde{Q}_{t_{i+1}} = \tilde{Q}_{t_i} + h\tilde{V}_{t_i} + \frac{1}{2}h^2\tilde{F}_{t_i}$;
- 8 Update velocity $\tilde{V}_{t_{i+1}} = \tilde{V}_{t_i} + h\tilde{F}_{t_i}$;
- 9 **end**

Output: Next state of the chain $X_1 = \tilde{Q}_{t_n}$.

A main result of this paper states that uHMC with sMC time integration produces an ε -accurate approximation of the target distribution using

$$O\left(\left(\frac{d}{K}\right)^{1/3} \left(\frac{L}{K}\right)^{5/3} \varepsilon^{-2/3} \log\left(\frac{\mathcal{W}^2(\mu, \nu)}{\varepsilon}\right)^+\right) \text{ gradient evaluations} \quad (5)$$

when initialized from an arbitrary distribution ν with finite second moment and run with the optimal hyperparameters detailed below. The proof of this complexity guarantee follows from two theorems, which we briefly describe.

Firstly, assuming that $LT^2 \leq 1/8$ and $h \leq T$, Theorem 6 uses a synchronous coupling of two copies of $\tilde{\pi}$ to demonstrate \mathcal{W}^2 -contractivity

$$\mathcal{W}^2(\nu\tilde{\pi}, \eta\tilde{\pi}) \leq e^{-c} \mathcal{W}^2(\nu, \eta) \quad \text{with } c = KT^2/6, \quad (6)$$

where ν, η are arbitrary probability measures on \mathbb{R}^d with finite second moment. The \mathcal{W}^2 -contraction coefficient e^{-c} has the nice feature that it is uniform in the time step size hyperparameter. The proof of Theorem 6 relies on almost sure contractivity of two realizations of the sMC time integrator starting with the same initial velocities and with synchronous random temporal sample points; see Lemma 5. The proof of this lemma crucially relies on K -strong convexity of U and the co-coercivity of ∇U ; see Remark 4 for background on the latter. The proof involves a careful balance of these competing effects at the random positions where the force is evaluated. We emphasize that an analogous \mathcal{W}^2 -contractivity result can be proven for uHMC with Verlet time integration without assuming higher regularity [3, Chapter 5]. As a corollary, $\tilde{\pi}$ admits a unique invariant measure $\tilde{\mu}$, but in general, due to time discretization bias $\tilde{\mu} \neq \mu$.

Secondly, we upper bound the \mathcal{W}^2 -asymptotic bias of $\tilde{\pi}$, which quantifies $\mathcal{W}^2(\mu, \tilde{\mu})$. To this end, let π denote the transition kernel of exact HMC, which uses the exact Hamiltonian flow per transition step and satisfies $\mu\pi = \mu$. Theorem 9 uses a coupling of $\tilde{\pi}$ and π to prove: for $LT^2 \leq 1/8$ and $h \leq T$,

$$\mathcal{W}^2(\mu, \tilde{\mu}) \leq 142 d^{1/2} c^{-1} (L/K)^{1/2} L^{1/4} h^{3/2}. \quad (7)$$

Remarkably, this upper bound only requires the assumption that U is L -gradient Lipschitz and K -strongly convex. The proof of Theorem 9 rests on the proof of L^2 -accuracy of the sMC integration scheme in Lemma 7.

Note the improvement in the \mathcal{W}^2 -asymptotic bias over uHMC with Verlet time integration, which in the absence of higher regularity is only first-order accurate. This improvement can be understood via the classical Fundamental Theorem of L^2 -Convergence of Strong Numerical Methods for SDEs [34, Theorem 1.1.1]. This theorem highlights that the expansion of the squared L^2 -error of a stochastic numerical method can lead to cancellations (to leading order) of cross terms. For strong numerical methods for SDEs, this cancellation (to leading order) of cross terms occurs because of the independence of the Brownian increments used at each integration step. Consequently, the expectation of cross terms that involve the Brownian increments can vanish to leading order because they have zero mean. For the sMC time integrator, a similar cancellation (to leading order) can occur, which is analogously due to independence of the sequence of random temporal sample points. Specifically, what happens is that the random potential force \tilde{F}_{t_i} appearing in the expectation of cross terms turns into an average of the potential force over the i -th stratum, which confers higher accuracy in these cross-terms. Turning this heuristic argument into a rigorous proof relies crucially on comparison to a ‘semi-exact’ flow, which uses the mean of \tilde{F}_{t_i} to update the position and velocity; see Lemmas 13 and 14 for details. The semi-exact flow is somewhat related to the Average Vector Field (AVF) method [37], which suggests that sMC might also be a useful tool for AVF.

To obtain the stated complexity guarantee, the choice of hyperparameters is optimized as follows. For clarity, numerical prefactors are suppressed here, but are fully worked out in Theorem 10 and Remark 11. Consider uHMC with sMC time integration initialized from a distribution ν with finite second moment and operated with hyperparameters satisfying:

$$\begin{aligned} \text{duration } T &\propto L^{-1/2}, \quad \text{time step size } h \propto (\varepsilon d^{-1/2} c(L/K)^{-1/2} L^{-1/4})^{2/3}, \text{ and} \\ \# \text{ of uHMC transition steps } m &\propto c^{-1} \log(\mathcal{W}^2(\mu, \nu)/\varepsilon)^+. \end{aligned}$$

With this selection of hyperparameters, the \mathcal{W}^2 -contraction rate in (6) reduces to $c \propto K/L$, and we find that

$$\begin{aligned} \mathcal{W}^2(\nu \tilde{\pi}^m, \mu) &\leq \mathcal{W}^2(\nu \tilde{\pi}^m, \tilde{\mu}) + \mathcal{W}^2(\tilde{\mu}, \mu) \\ &\stackrel{(6)}{\leq} e^{-cm} \mathcal{W}^2(\nu, \tilde{\mu}) + \mathcal{W}^2(\tilde{\mu}, \mu) \leq e^{-cm} \mathcal{W}^2(\nu, \mu) + 2\mathcal{W}^2(\tilde{\mu}, \mu) \stackrel{(7)}{\leq} \varepsilon. \end{aligned}$$

Therefore, with the above choice of hyperparameters, we find the total number of gradient evaluations to be $m \times T/h$ — as stated in (5).

1.3. Why duration randomization?

So far, we have summarized the benefit of time integration randomization for uHMC with complete momentum refreshment. Motivated by the findings of Monmarché [35], it is interesting to develop corresponding results for the case of uHMC with partial momentum refreshment. Since after a random number of uHMC transition steps with partial momentum refreshment a complete velocity refreshment occurs, one can equivalently consider uHMC with duration randomization, as in the randomized uHMC process introduced in §6 of [7].

This duration-randomized uHMC process is a fully implementable pure jump process on phase space \mathbb{R}^{2d} that iterates between two types of jumps: (i) a single step of a time integrator for the Hamiltonian dynamics; or (ii) a complete momentum refreshment. There are again two hyperparameters entering the algorithm: a time step hyperparameter h and a mean duration hyperparameter λ^{-1} . Importantly, because the duration-randomized uHMC process admits an infinitesimal generator, this process is amenable to detailed contractivity and asymptotic bias analyses.

Theorem 17 states that the \mathcal{W}^2 -contraction rate of this randomized uHMC process on phase space is $\gamma = K\lambda^{-1}/10$. The proof of this theorem is based on a synchronous coupling of two copies of the randomized uHMC process. If the duration hyperparameters are selected optimally, then the contraction rate becomes $\gamma \propto K^{1/2}(K/L)^{1/2}$. At first glance, this rate looks better than the corresponding rate for non-duration randomized uHMC, i.e., $c \propto K/L$. However, viewed on the same infinitesimal time scale, these rates are essentially identical in the sense that $c/T \propto \gamma$. Therefore, duration randomization does not lead to an improvement in terms of contractivity.

So then what is the benefit of duration randomization? A reason may be found in the asymptotic bias. To quantify the asymptotic bias, a coupling of the duration-randomized uHMC process with an ‘exact’ counterpart is considered. This coupling is itself a jump process with generator \mathcal{A}^C defined in (67). This coupling admits a Foster-Lyapunov function given by a quadratic ‘distorted’ metric on phase space [1]; this function ρ^2 is defined in (59). In particular, the coupling satisfies the following infinitesimal drift condition

$$\mathcal{A}^C \rho(y)^2 \leq -\frac{\gamma}{2} \rho(y)^2 + \frac{1}{2} \left(1 + \frac{1}{K\lambda^{-2}}\right) (L^{3/2}h|x|^2 + |v|^2) Lh^3,$$

for all $y = ((x, v), (\tilde{x}, \tilde{v})) \in \mathbb{R}^{4d}$. By Itô’s formula for jump processes, the corresponding finite-time drift condition is used in Theorem 19 to quantify the \mathcal{W}^2 -asymptotic bias of the duration-randomized uHMC process. Choosing the hyperparameters optimally, an improvement in the complexity of the randomized uHMC process is found; see Remark 20 for details. The improvement in complexity due to duration randomization is analogous to the improvement found by time integration randomization. Indeed, in both cases randomization leads to an improvement in the \mathcal{W}^2 -asymptotic bias. For time integration randomization, this can be traced back to an improvement in the finite-time L^2 -accuracy of the sMC time integrator. For duration randomization, the improvement is due to how the time discretization errors accumulate over an infinite-time interval.

We remark that in the presence of higher regularity (e.g., U is Hessian Lipschitz), a modification of the sMC scheme that recruits an antithetic sample point per integration step is expected to be $O(h^{5/2})$ L^2 -accurate. Thus, for the purpose of unadjusted Hamiltonian MCMC, a randomized time integrator is generally preferable to Verlet time integration.

Ideas for future work include (i) develop contractivity and asymptotic bias estimates in total variation distance for uHMC with sMC time integration by means of one-shot couplings [5]; (ii) incorporate time integration randomization into adjusted HMC and extend the conductance-type argument in [12] to obtain a complexity guarantee under weaker regularity conditions than for adjusted HMC with Verlet; and (iii) combine randomized time integration with time step or duration hyperparameter adaptivity to deal with multiscale features in the target distribution — as in [28, 25, 24].

Acknowledgements

We wish to acknowledge Persi Diaconis for his support and encouragement of this collaboration. We also acknowledge Bob Carpenter, Tore Kleppe, Pierre Monmarché, Stefan Oberdörster, and Lihan Wang for feedback on a previous version of this paper. N. Bou-Rabee has been supported by the National Science Foundation under Grant No. DMS-2111224. M. Marsden also acknowledges his advisors Persi Diaconis and Lexing Ying for their support.

2. uHMC with sMC time integration

2.1. Notation

Let $\mathcal{P}(\mathbb{R}^d)$ denote the set of all probability measures on \mathbb{R}^d , and denote by $\mathcal{P}^p(\mathbb{R}^d)$ the subset of probability measures on \mathbb{R}^d with finite p -th moment. Denote the set of all couplings of $\nu, \eta \in \mathcal{P}(\mathbb{R}^d)$ by $\text{Couplings}(\nu, \eta)$. For $\nu, \eta \in \mathcal{P}(\mathbb{R}^d)$, define the L^p -Wasserstein distance by

$$\mathcal{W}^p(\nu, \eta) := \left(\inf \left\{ E[|X - Y|^p] : \text{Law}(X, Y) \in \text{Couplings}(\nu, \eta) \right\} \right)^{1/p}.$$

2.2. Definition of the uHMC Algorithm with sMC time integration

Unadjusted Hamiltonian Monte Carlo (uHMC) is an MCMC method for approximate sampling from a ‘target’ probability distribution on \mathbb{R}^d of the form

$$\mu(dx) = \mathcal{Z}^{-1} \exp(-U(x)) dx, \quad \mathcal{Z} = \int_{\mathbb{R}^d} \exp(-U(x)) dx, \quad (8)$$

where $U : \mathbb{R}^d \rightarrow \mathbb{R}_{\geq 0}$ is assumed to be a continuously differentiable function such that $\mathcal{Z} < \infty$. The function U is termed ‘potential energy’ and $-\nabla U$ is termed ‘potential force’ since it is a force derivable from a potential.

The standard uHMC algorithm with complete velocity refreshment generates a Markov chain on \mathbb{R}^d with the help of: (i) a deterministic Verlet time integrator for the Hamiltonian dynamics corresponding to the unit mass Hamiltonian $H(x, v) = (1/2)|v|^2 + U(x)$; and (ii) an i.i.d. sequence of random initial velocities $(\xi^k)_{k \in \mathbb{N}_0} \stackrel{i.i.d.}{\sim} \mathcal{N}(0, I_d)$. To be sure, there are only two hyperparameters that need to be specified in this algorithm: the duration $T > 0$ of the Hamiltonian dynamics and the time-step-size $h \geq 0$; and for simplicity of notation, we often assume $T/h \in \mathbb{Z}$ when $h > 0$, which implies that $h \leq T$. Let $\{t_k := kh\}_{k \in \mathbb{N}_0}$ be an evenly spaced time grid. This grid partitions time into subintervals $\{[t_k, t_{k+1}]\}_{k \in \mathbb{N}_0}$ termed ‘strata’.

In the $(k+1)$ -th uHMC transition step, a deterministic Verlet time integration is performed with initial position given by the k -th step of the chain and initial velocity given by ξ^k . The $(k+1)$ -th state of the chain is then the final position computed by Verlet. Verlet integrates the Hamiltonian dynamics by using: (i) a piecewise quadratic approximation of positions which can be interpolated by a quadratic function of time on each stratum $[t_i, t_{i+1}]$; and (ii) a deterministic trapezoidal quadrature rule of the time integral of the potential force over each stratum $[t_i, t_{i+1}]$ to update the velocities.

However, since in uHMC we are almost exclusively interested in a stochastic notion of accuracy of the numerical time integration [8, Theorem 3.6], it is quite natural to instead use a randomized time integrator for the Hamiltonian dynamics.¹ The aim of this paper is to suggest one such randomized integration

¹More generally, a stochastic notion of accuracy is an apt concept for inexact MCMC [19].

strategy, which involves a very minor modification of the Verlet time integrator, and hence, is easy to implement. The basic idea in this new integrator is to replace the trapezoidal quadrature rule used by Verlet in each stratum with a Monte Carlo quadrature rule. Note that this construction substantially relaxes the regularity requirements on the potential force. The resulting integration scheme is an instance of a stratified Monte Carlo (sMC) time integrator.

To precisely define this variant of uHMC, in addition to the random initial velocities we define an independent sequence of sequences $(\mathcal{U}_i^k)_{i,k \in \mathbb{N}_0}$ whose terms are independent uniform random variables $\mathcal{U}_i^k \sim \text{Uniform}(t_i, t_{i+1})$. In the $(k+1)$ -th transition step of uHMC, a discrete solution is computed from an initial state $(x, v) \in \mathbb{R}^{2d}$ that we interpolate by the *sMC flow* $(\tilde{Q}_t^k(x, v), \tilde{V}_t^k(x, v))$ which satisfies

$$\frac{d}{dt} \tilde{Q}_t^k = \tilde{V}_t^k, \quad \frac{d}{dt} \tilde{V}_t^k = -\nabla U(\tilde{Q}_{[t]_h}^k + (\tau_t^k - [t]_h) \tilde{V}_{[t]_h}^k) \quad (9)$$

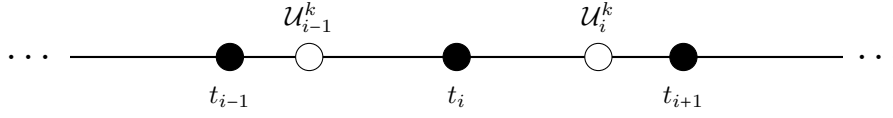
where we introduced the floor (resp. ceiling) function to the nearest time grid point less (resp. greater) than time t , i.e.,

$$[t]_h = \max\{s \in h\mathbb{Z} : s \leq t\}, \quad \lceil t \rceil_h = \min\{s \in h\mathbb{Z} : s \geq t\} \quad \text{for } h > 0, \quad (10)$$

and the random temporal point in the i -th stratum

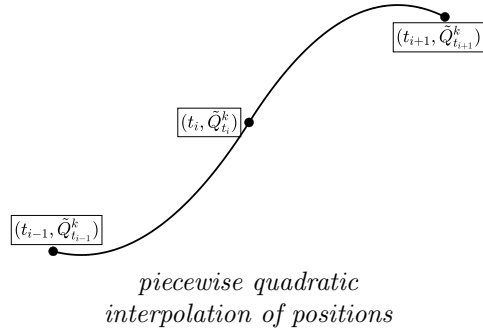
$$\tau_t^k = \mathcal{U}_i^k \quad \text{for } t \in [t_i, t_{i+1}),$$

as illustrated below.



As a shorthand, let $\tilde{F}_{t_i}^k := -\nabla U(\tilde{Q}_{t_i}^k + (\mathcal{U}_i^k - t_i) \tilde{V}_{t_i}^k)$ be the potential force evaluated at the random temporal point in the i -th stratum.

By integrating (9), note that \tilde{Q}_t^k is a piecewise quadratic function of time that interpolates between the points $\{\tilde{Q}_{t_i}^k\}$ and satisfies $\frac{d}{dt} \tilde{Q}_t^k = \tilde{V}_t^k$ and $\frac{d^2}{dt^2} \tilde{Q}_t^k \Big|_{t=t_i+} = \tilde{F}_{t_i}^k$, while \tilde{V}_t^k is a piecewise linear function of time that interpolates between $\{\tilde{V}_{t_i}^k\}$.



For $h = 0$, we set $[t]_h = \lceil t \rceil_h = t$, drop the tildes in the notation, and since the corresponding flow is deterministic, we use lower case letters $(q_t(x, v), v_t(x, v))$

to denote the *exact flow* which satisfies

$$\frac{d}{dt}q_t = v_t, \quad \frac{d}{dt}v_t = -\nabla U(q_t). \quad (11)$$

On the time grid points, the sMC flow is an unbiased estimator for the *semi-exact flow* $(\bar{q}_t(x, v), \bar{v}_t(x, v))$ which satisfies:

$$\frac{d}{dt}\bar{q}_t = \bar{v}_t, \quad \frac{d}{dt}\bar{v}_t = -\frac{1}{h} \int_{[t]_h}^{\lceil t \rceil_h+h} \nabla U(\bar{q}_{[t]_h} + (s - [t]_h)\bar{v}_{[t]_h}) ds. \quad (12)$$

The semi-exact flow plays a crucial role in §2.5 to quantify the L^2 -accuracy of the sMC flow with respect to the exact flow.

With this notation, the chain $(\tilde{X}^k)_{k \in \mathbb{N}_0}$ corresponding to uHMC with sMC time integration of the Hamiltonian dynamics is defined as follows.

Definition 1 (uHMC with sMC time integration). *Given an initial state $x \in \mathbb{R}^d$, a duration hyperparameter $T > 0$, and time step size hyperparameter $h \geq 0$ with $T/h \in \mathbb{Z}$ for $h > 0$, define $\tilde{X}^0(x) := x$ and*

$$\tilde{X}^{k+1}(x) := \tilde{Q}_T^k(\tilde{X}^k(x), \xi^k) \quad \text{for } k \in \mathbb{N}_0.$$

Let $\tilde{\pi}(x, A) = P[\tilde{X}^1(x) \in A]$ denote the corresponding one-step transition kernel.

For $h = 0$, we recover *exact HMC*. In this case, we drop all tildes in the notation, i.e., the k -th transition step is denoted by $X^k(x)$, and the corresponding transition kernel is denoted by π . The target measure μ is invariant under π , because the exact flow preserves the Boltzmann-Gibbs probability measure on \mathbb{R}^{2d} with density proportional to $\exp(-H(x, v))$, and μ is the first marginal of this measure. When $h > 0$, and under certain conditions (detailed next), $\tilde{\pi}$ has a unique invariant probability measure denoted by $\tilde{\mu}$, which typically approaches μ as $h \searrow 0$. In the sequel, uHMC refers to *uHMC with sMC time integration*.

2.3. Assumptions

To prove our main results, we assume the following.

Assumption 2. *The potential energy function $U : \mathbb{R}^d \rightarrow \mathbb{R}$ is continuously differentiable and satisfies the following conditions:*

A.1 *U has a global minimum at 0 and $U(0) = 0$.*

A.2 *U is L -gradient Lipschitz continuous, i.e., there exists $L > 0$ such that*

$$|\nabla U(x) - \nabla U(y)| \leq L|x - y| \quad \text{for all } x, y \in \mathbb{R}^d.$$

A.3 *U is K -strongly convex, i.e., there exists $K > 0$ such that*

$$(\nabla U(x) - \nabla U(y)) \cdot (x - y) \geq K|x - y|^2 \quad \text{for all } x, y \in \mathbb{R}^d.$$

Assumptions **A.1-A.3** imply \mathcal{W}^2 -contractivity of the transition kernel of uHMC; see Theorem 6 below. By the Banach fixed point theorem, contractivity implies existence of a unique invariant probability measure of $\tilde{\pi}$ [3, Theorem 2.9]. The \mathcal{W}^2 -asymptotic bias of this invariant measure is upper bounded in Theorem 9.

Remark 3. Under **A.1-A.3**, using a quadratic Foster-Lyapunov function argument², it can be shown that the target distribution satisfies

$$\int_{\mathbb{R}^d} |x| \mu(dx) \leq \left(\int_{\mathbb{R}^d} |x|^2 \mu(dx) \right)^{1/2} \leq d^{1/2} / K^{1/2}$$

where in the first step we used Jensen's inequality. The bound is sharp since it is attained by a centered Gaussian random variable ξ with $E|\xi|^2 = d/K$.

Remark 4. If U is continuously differentiable, convex, and L -gradient Lipschitz, then ∇U satisfies the following 'co-coercivity' property

$$|\nabla U(x) - \nabla U(y)|^2 \leq L (\nabla U(x) - \nabla U(y)) \cdot (x - y), \quad \text{for all } x, y \in \mathbb{R}^d. \quad (13)$$

This property plays a crucial role in proving a sharp \mathcal{W}^2 -contraction coefficient for the uHMC transition kernel in the globally strongly convex setting.

2.4. L^2 -Wasserstein Contractivity

Let $(\tilde{Q}_t(x, v), \tilde{V}_t(x, v))$ be a realization of the sMC flow satisfying (9) from the initial condition $(x, v) \in \mathbb{R}^{2d}$ with a random sequence of independent temporal sample points $(\mathcal{U}_i)_{i \in \mathbb{N}_0}$ such that $\mathcal{U}_i \sim \text{Uniform}(t_i, t_{i+1})$. When U is K -strongly convex and L -gradient Lipschitz, the exact flow from different initial positions but synchronous initial velocities is itself contractive if $LT^2 \leq 1/4$ [13, Lemma 6].³ Analogously, if $LT^2 \leq 1/8$ and the time step size additionally satisfies $h \leq T$ (which follows from the hypothesis that $T/h \in \mathbb{Z}$), the following lemma states that $|\tilde{Q}_T(x, v) - \tilde{Q}_T(y, v)|^2$ is almost surely contractive.

Lemma 5 (Almost Sure Contractivity of sMC Time Integrator from Synchronized Velocities). *Suppose that **A.1-A.3** hold. Let $T > 0$ satisfy:*

$$LT^2 \leq 1/8, \quad (14)$$

and $h \geq 0$ satisfy $T/h \in \mathbb{Z}$ if $h > 0$. Then for all $x, y, v \in \mathbb{R}^d$,

$$|\tilde{Q}_T(x, v) - \tilde{Q}_T(y, v)|^2 \leq (1 - KT^2/3) |x - y|^2 \quad \text{almost surely}. \quad (15)$$

The proof of Lemma 5 is deferred to Section 2.7. By synchronously coupling both the random initial velocities and the random temporal sample points in two copies of uHMC starting at different initial conditions, and applying Lemma 5, we obtain the following.

²See Proposition 1(ii) of [20].

³Under $LT^2 \leq \min(1/4, K/L)$, Mangoubi and Smith first obtained a similar result [31].

Theorem 6 (\mathcal{W}^2 -Contractivity of uHMC under global strong convexity). *Suppose that [A.1-A.3](#) hold. Let $T > 0$ and $h \geq 0$ be such that [\(14\)](#) holds with $T/h \in \mathbb{Z}$ if $h > 0$. Then for any pair of probability measures $\nu, \eta \in \mathcal{P}^2(\mathbb{R}^d)$,*

$$\begin{aligned} \mathcal{W}^2(\nu \tilde{\pi}^m, \eta \tilde{\pi}^m) &\leq (1-c)^m \mathcal{W}^2(\nu, \eta) \quad \text{where} & (16) \\ c &= KT^2/6. & (17) \end{aligned}$$

Note that the \mathcal{W}^2 -contraction coefficient in [Theorem 6](#) is uniform in the time step size hyperparameter, and as $h \searrow 0$, recovers (up to a numerical pre-factor) the sharp \mathcal{W}^2 -contraction coefficient of exact HMC.

2.5. L^2 -Wasserstein Asymptotic Bias

As emphasized in previous works [\[8, 19\]](#), an apt notion of accuracy of the underlying time integrator in unadjusted Hamiltonian Monte Carlo (and other inexact MCMC methods) is a stochastic one, e.g., L^2 -accuracy. Remarkably, the sMC time integrator is 3/2-order L^2 -accurate without higher regularity assumptions such as Lipschitz continuity of the Hessian of U .

Lemma 7 (L^2 -accuracy of sMC Time Integrator). *Suppose that [A.1-A.2](#) hold. Let $T > 0$ satisfy $LT^2 \leq 1/8$, and let $h > 0$ satisfy $T/h \in \mathbb{Z}$. Then for any $x \in \mathbb{R}^d$ and $k \in \mathbb{N}_0$ such that $t_k \leq T$,*

$$\left(E \left[|\tilde{Q}_{t_k}(x, v) - q_{t_k}(x, v)|^2 \right] \right)^{1/2} \leq 71 (|v| + \sqrt{L}|x|) L^{1/4} h^{3/2}. \quad (18)$$

Note that [A.3](#) is not assumed in [Lemma 7](#). The 3/2-order of L^2 -accuracy of the sMC time integrator is numerically verified in [Figure 2](#).

Proof of Lemma 7. The proof of L^2 -accuracy of the sMC integrator is carried out in two steps. First, the sMC flow is compared to the semi-exact flow in [Lemma 13](#). Then, the semi-exact flow is compared to the exact flow in [Lemma 14](#). An application of the triangle inequality, the bound $L^{1/4}h^{1/2} \leq 1/\sqrt{2}$ and the evaluation of the exponentials gives the required result. \square

Remark 8. *The 3/2-order of L^2 -accuracy of the sMC time integrator is reminiscent of the classical Fundamental Theorem for L^2 -Convergence of Strong Numerical Methods for SDEs, which roughly states: if $p_1 \geq p_2 + 1/2$ and $p_2 > 1/2$ are the order of mean and mean-square accuracy (respectively), then the L^2 -accuracy of the method is order $p_2 - 1/2$ [\[34, Theorem 1.1.1\]](#). This is due to cancellations (to leading order) in the L^2 error expansion, due to independence of the Brownian increments. Here the cancellations (to leading order) occur because of independence of the sequence of random temporal sample points used by the sMC time integrator. A rigorous proof expanding on this heuristic is given in [Section 2.9](#).*

Additionally, assuming [A.3](#) holds, using a triangle inequality trick [[33](#), Remark 6.3], the L^2 -accuracy bound in Lemma [7](#) combined with Theorem [6](#) can be used to bound the \mathcal{W}^2 -asymptotic bias, i.e., $\mathcal{W}^2(\mu, \tilde{\mu})$.

Theorem 9. *Suppose that [A.1-A.3](#) hold. Let $T > 0$ and $h \geq 0$ be such that [\(14\)](#) holds with $T/h \in \mathbb{Z}$ if $h > 0$. Additionally, assume $LT^2 \leq 1/8$. Then*

$$\mathcal{W}^2(\mu, \tilde{\mu}) \leq 142 d^{1/2} c^{-1} (L/K)^{1/2} L^{1/4} h^{3/2}. \quad (19)$$

Proof. By the triangle inequality,

$$\begin{aligned} \mathcal{W}^2(\mu, \tilde{\mu}) &= \mathcal{W}^2(\mu\pi, \tilde{\mu}\tilde{\pi}) \leq \mathcal{W}^2(\mu\pi, \mu\tilde{\pi}) + \mathcal{W}^2(\mu\tilde{\pi}, \tilde{\mu}\tilde{\pi}) \\ &\stackrel{\text{Thm. 6}}{\leq} \mathcal{W}^2(\mu\pi, \mu\tilde{\pi}) + (1-c)\mathcal{W}^2(\mu, \tilde{\mu}) \implies \mathcal{W}^2(\mu, \tilde{\mu}) \leq c^{-1}\mathcal{W}^2(\mu\pi, \mu\tilde{\pi}). \end{aligned}$$

Employing now Lemma [7](#), Remark [3](#), $\xi \sim \mathcal{N}(0, I_d)$, the triangle inequality and the fact $L/K \geq 1$ gives the required result. \square

2.6. Complexity Guarantee

In sum, Theorem [6](#) implies, for any $\nu \in \mathcal{P}^2(\mathbb{R}^d)$, $\mathcal{W}^2(\tilde{\mu}, \nu\tilde{\pi}^m) \leq e^{-cm}\mathcal{W}^2(\tilde{\mu}, \nu)$; and Theorem [9](#) implies $\mathcal{W}^2(\mu, \tilde{\mu}) \leq O(h^{3/2})$. Together these two results imply $\mathcal{W}^2(\mu, \nu\tilde{\pi}^m)$ can be made arbitrarily small by choosing h sufficiently small and m large enough. This complexity argument is standard for inexact MCMC methods [[19](#), [8](#)], but we briefly summarize it here for completeness.

Theorem 10. *Suppose that [A.1-A.3](#) hold. Let $T > 0$ and $h \geq 0$ be such that [\(14\)](#) holds with $T/h \in \mathbb{Z}$ if $h > 0$. Let $\nu \in \mathcal{P}^2(\mathbb{R}^d)$. Define $\Delta(m) := \mathcal{W}^2(\mu, \nu\tilde{\pi}^m)$, i.e., the L^2 Wasserstein distance to the target measure μ after m steps of uHMC. For any $\varepsilon > 0$, suppose that $h \geq 0$ and $m \in \mathbb{N}$ satisfy*

$$m \geq m^* := c^{-1} \log(2\mathcal{W}^2(\mu, \nu)/\varepsilon)^+, \quad h \leq h^* := e^{-4} \left(\frac{c(\varepsilon/2)}{d^{1/2}(L/K)^{1/2}L^{1/4}} \right)^{2/3}.$$

Then $\Delta(m) \leq \varepsilon$.

Proof. Let $m \geq m^*$ and $h \leq h^*$. By the triangle inequality,

$$\begin{aligned} \Delta(m) &\leq \mathcal{W}^2(\mu, \tilde{\mu}) + \mathcal{W}^2(\tilde{\mu}, \nu\tilde{\pi}^m) \stackrel{\text{Thm. 6}}{\leq} \mathcal{W}^2(\mu, \tilde{\mu}) + e^{-cm}\mathcal{W}^2(\tilde{\mu}, \nu) \\ &\leq 2\mathcal{W}^2(\mu, \tilde{\mu}) + e^{-cm}\mathcal{W}^2(\mu, \nu) \stackrel{\text{Thm. 9}}{\leq} e^6 d^{1/2} c^{-1} \left(\frac{L}{K} \right)^{1/2} L^{1/4} h^{3/2} + e^{-cm}\mathcal{W}^2(\mu, \nu). \end{aligned}$$

Since $m \geq m^*$ and $h \leq h^*$, the required result follows. \square

Remark 11 (Complexity Guarantee). *For any accuracy $\varepsilon > 0$, Theorem [10](#) states that $m \geq m^*$ uHMC transition steps with $h \leq h^*$ guarantee that $\Delta(m) < \varepsilon$. To turn this into a complexity guarantee, we specify the duration hyperparameter, and in turn, estimate the corresponding # of gradient evaluations. In particular, if one chooses the duration T to saturate the condition $LT^2 \leq 1/8$ in [\(14\)](#),*

i.e., $T = L^{-1/2}/8$, then the \mathcal{W}^2 -contraction coefficient reduces to $c = 48^{-1}K/L$. Since each uHMC transition step involves T/h gradient evaluations, the corresponding # of gradient evaluations is therefore

$$(m \text{ uHMC transition steps}) \times (T/h \text{ sMC integration steps}) = 8^{7/6} \cdot 6^{5/3} \cdot e^4 \left(\frac{d}{K}\right)^{1/3} \left(\frac{L}{K}\right)^{5/3} \left(\frac{\varepsilon}{2}\right)^{-2/3} \log\left(\frac{2\mathcal{W}^2(\mu, \nu)}{\varepsilon}\right)^+.$$

2.7. Proof of L^2 -Wasserstein contractivity

This proof carefully adapts ideas from [8] and Lemma 6 of [13]. The main idea in the proof is to carefully balance two competing effects at the random temporal sample points where the potential force is evaluated: (i) strong convexity of U (A.3); and (ii) co-coercivity of ∇U (Remark 13).

Proof of Lemma 5. Let $t \in [0, T]$. Introduce the shorthands

$$\begin{aligned} x_t &:= \tilde{Q}_{[t]_h}(x, v) + (\tau_t - [t]_h)\tilde{V}_{[t]_h}(x, v), \quad \text{and} \\ y_t &:= \tilde{Q}_{[t]_h}(y, v) + (\tau_t - [t]_h)\tilde{V}_{[t]_h}(y, v), \end{aligned} \quad (20)$$

where recall that $\tau_t = \mathcal{U}_i$ for $t \in [t_i, t_{i+1})$ and $(\mathcal{U}_k)_{k \in \mathbb{N}_0}$ is a sequence of independent random variables such that $\mathcal{U}_i \sim \text{Uniform}(t_i, t_{i+1})$. Let $z_t := x_t - y_t$,

$$Z_t := \tilde{Q}_t(x, v) - \tilde{Q}_t(y, v), \quad \text{and} \quad W_t := \tilde{V}_t(x, v) - \tilde{V}_t(y, v).$$

Let $A_t := |Z_t|^2$, $B_t := 2Z_t \cdot W_t$ and $a_t := |z_t|^2$. Our goal is to obtain an upper bound for A_t . To this end, define

$$\rho_t := \phi_t \cdot z_t, \quad \phi_t := \nabla U(x_t) - \nabla U(y_t),$$

and note that by A.2, A.3 and (13),

$$K a_t \stackrel{\text{A.3}}{\leq} \rho_t \stackrel{\text{A.2}}{\leq} L a_t, \quad |\phi_t|^2 \stackrel{(13)}{\leq} L \rho_t, \quad \text{for all } t \geq 0. \quad (21)$$

In (21), we underscore that the inequalities take place at the random positions (x_t, y_t) in (20) where the potential force is evaluated. By (9), note that

$$\frac{d}{dt} Z_t = W_t, \quad \frac{d}{dt} W_t = -\phi_t, \quad (22)$$

As a consequence of (22), a short computation shows that A_t and B_t satisfy:

$$\frac{d}{dt} A_t = B_t, \quad \frac{d}{dt} B_t = -K A_t + 2|W_t|^2 + \epsilon_t, \quad (23)$$

where $\epsilon_t := K A_t - 2Z_t \cdot \phi_t$. Introduce the shorthand notation

$$s_{t-r} := \frac{\sin(\sqrt{K}(t-r))}{\sqrt{K}}, \quad \text{and} \quad c_{t-r} := \cos(\sqrt{K}(t-r)),$$

which satisfy $c_{t-r} = -\frac{d}{dr} s_{t-r}$. By variation of parameters,

$$A_T = c_T A_0 + \int_0^T s_{T-r} (2|W_r|^2 + \epsilon_r) dr. \quad (24)$$

To upper bound the integral involving $|W_r|^2$ in (24), use (22) and note that $W_0 = 0$, since the initial velocities in the two copies are synchronized. Therefore,

$$|W_t|^2 = \left| \int_0^t \phi_s ds \right|^2 \leq t \int_0^t |\phi_s|^2 ds \leq Lt \int_0^t \rho_s ds \quad (25)$$

where in the second step we used Cauchy-Schwarz, and in the last step, we used (21). Since s_{t-r} is monotonically decreasing with r ,

$$0 \leq s_{t-r} \leq s_{t-s}, \quad \text{for } s \leq r \leq t \leq \frac{\pi/2}{\sqrt{K}}. \quad (26)$$

Therefore, combining these bounds and by Fubini's Theorem, note that

$$\begin{aligned} \int_0^t s_{t-r} |W_r|^2 dr &\stackrel{(25)}{\leq} L \int_0^t \int_0^r r s_{t-r} \rho_s ds dr \\ &\stackrel{(26)}{\leq} L \int_0^t \int_0^r r s_{t-s} \rho_s ds dr \\ &\leq L \int_0^t \int_s^t r s_{t-s} \rho_s dr ds \leq (Lt^2/2) \int_0^t s_{t-s} \rho_s ds. \end{aligned}$$

In fact, as a byproduct of this calculation, observe that

$$\left(\int_0^t s_{t-r} |W_{[r]_h}|^2 dr \right) \vee \left(\int_0^t s_{t-r} |W_r|^2 dr \right) \leq (Lt^2/2) \int_0^t s_{t-s} \rho_s ds. \quad (27)$$

To upper bound the integral involving ϵ_r in (24), rewrite it as

$$\begin{aligned} \epsilon_t &= K A_t - 2\rho_t - 2(t - \tau_t) W_{[t]_h} \cdot \phi_t + (t - [t]_h)^2 |\phi_t|^2 \\ &= K a_t - 2\rho_t - 2(t - \tau_t) W_{[t]_h} \cdot \phi_t + (t - [t]_h)^2 |\phi_t|^2 \\ &\quad + K \left| (t - \tau_t) W_{[t]_h} - \frac{(t - [t]_h)^2}{2} \phi_t \right|^2 + 2K \left((t - \tau_t) W_{[t]_h} - \frac{(t - [t]_h)^2}{2} \phi_t \right) \cdot z_t \\ &\stackrel{(21)}{\leq} K a_t - 2\rho_t - 2(t - \tau_t) W_{[t]_h} \cdot \phi_t + (t - [t]_h)^2 |\phi_t|^2 \\ &\quad + K \left| (t - \tau_t) W_{[t]_h} - \frac{(t - [t]_h)^2}{2} \phi_t \right|^2 + 2K (t - \tau_t) W_{[t]_h} \cdot z_t \\ &\leq -2\rho_t + K(1 + Kh^2) a_t + (2h^2 + Kh^4/2) |\phi_t|^2 + 2(1 + Kh^2) |W_{[t]_h}|^2 \end{aligned} \quad (28)$$

where in the last step we used Cauchy-Schwarz and Young's product inequality.

Inserting these bounds into the second term of (24) yields

$$\begin{aligned}
& \int_0^T s_{T-r} (2|W_r|^2 + \epsilon_r) dr \\
& \stackrel{(28)}{\leq} \int_0^T s_{T-r} (2|W_r|^2 + 2(1 + Kh^2)|W_{[r]_h}|^2 - 2\rho_r + (2h^2 + Kh^4/2)|\phi_r|^2 \\
& \quad + K(1 + Kh^2)a_r) dr \\
& \stackrel{(27)}{\leq} \int_0^T s_{T-r} ([LT^2(2 + Kh^2) - 2]\rho_r + (2h^2 + Kh^4/2)|\phi_r|^2 \\
& \quad + K(1 + Kh^2)a_r) dr \\
& \stackrel{(21)}{\leq} \int_0^T s_{T-r} ([Lh^2(2 + Kh^2/2) + LT^2(2 + Kh^2) - 2]\rho_r \\
& \quad + K(1 + Kh^2)a_r) dr, \\
& \stackrel{(21)}{\leq} K \int_0^T s_{T-r} [Lh^2(2 + Kh^2/2) + LT^2(2 + Kh^2) - 2 + (1 + Kh^2)] a_r dr.
\end{aligned}$$

where in the last step we used that $K \leq L$, $h \leq T$ (which follows from $T/h \in \mathbb{Z}$), and condition (14). In fact, this upper bound is non-positive, and therefore, this term can be dropped from (24) to obtain $A_T \leq c_T A_0$. The required estimate is then obtained by inserting the elementary inequality

$$\begin{aligned}
c_T & \leq 1 - (1/2)KT^2 + (1/6)K^2T^4 \\
& \leq 1 - (1/2)KT^2 + (1/48)KT^2(K/L) \leq 1 - (1/2 - 1/48)KT^2
\end{aligned}$$

which is valid by condition (14) and $K \leq L$. The required result holds because $1/2 - 1/48 = 23/48 > 1/3$. \square

2.8. A priori upper bounds for the Stratified Monte Carlo Integrator

The following a priori upper bounds for the sMC and semi-exact flows are useful to prove L^2 -accuracy of the sMC time integrator.

Lemma 12 (A priori bounds). *Suppose A.1-A.2 hold. Let $T > 0$ satisfy $LT^2 \leq 1/8$ and let $h \geq 0$ satisfy $T/h \in \mathbb{Z}$ if $h > 0$. For any $x, y, u, v \in \mathbb{R}^d$, we have almost surely*

$$\sup_{s \leq T} |\tilde{Q}_s(x, v)| \vee \sup_{s \leq T} |\tilde{q}_s(x, v)| \leq (1 + L(T^2 + Th)) \max(|x|, |x + Tv|), \quad (29)$$

$$\sup_{s \leq T} |\tilde{V}_s(x, v)| \vee \sup_{s \leq T} |\tilde{v}_s(x, v)| \leq |v| + LT(1 + L(T^2 + Th)) \max(|x|, |x + Tv|). \quad (30)$$

The proof of Lemma 12 is nearly identical to the proof of Lemma 3.1 of [6] and hence is omitted.

2.9. Proof of L^2 -Accuracy of sMC Integrator

The next two lemmas combined with the triangle inequality imply the L^2 -accuracy of the sMC time integrator given in Lemma 7.

Lemma 13 (L^2 -accuracy of sMC Time Integrator with respect to Semi-Exact Flow). *Suppose A.1-A.2 hold. Let $T > 0$ satisfy $LT^2 \leq 1/8$ and let $h > 0$ satisfy $T/h \in \mathbb{Z}$. Then for any $x \in \mathbb{R}^d$ and $k \in \mathbb{N}_0$ such that $t_k \leq T$,*

$$\left(E[|\tilde{Q}_{t_k}(x, v) - \bar{q}_{t_k}(x, v)|^2]\right)^{1/2} \leq \sqrt{2}e^{31/8}L^{1/4}(|v| + L^{1/2}|x|)h^{3/2}. \quad (31)$$

Lemma 14 (Accuracy of Semi-Exact Flow). *Suppose A.1-A.2 hold. Let $T > 0$ satisfy $LT^2 \leq 1/8$, and let $h > 0$ satisfy $T/h \in \mathbb{Z}$. Then for any $x, v \in \mathbb{R}^d$ and $k \in \mathbb{N}_0$ such that $t_k \leq T$,*

$$|\bar{q}_{t_k}(x, v) - q_{t_k}(x, v)| \leq 2e^{5/8}L^{1/2}(|v| + L^{1/2}|x|)h^2. \quad (32)$$

The proofs of these lemmas use the following discrete Grönwall inequality, which we include for the readers' convenience.

Lemma 15 (Discrete Grönwall inequality in Forward Difference Form). *Let $\lambda, h \in \mathbb{R}$ be such that $1 + \lambda h > 0$. Suppose that $(g_k)_{k \in \mathbb{N}_0}$ is a non-decreasing sequence, and $(a_k)_{k \in \mathbb{N}_0}$ satisfy $a_{k+1} \leq (1 + \lambda h)a_k + g_k$ for $k \in \mathbb{N}_0$. Then it holds*

$$a_k \leq (1 + \lambda h)^k a_0 + \frac{1}{\lambda h} ((1 + \lambda h)^k - 1) g_{k-1}, \quad \text{for all } k \in \mathbb{N}.$$

Proof of Lemma 13. Let $(\tilde{Q}_t(x, v), \tilde{V}_t(x, v))$ be a realization of the sMC time integrator from the initial condition $(x, v) \in \mathbb{R}^{2d}$ which satisfies (9). A key ingredient in this proof are the a priori upper bounds in Lemma 12. In particular, since $L(T^2 + Th) \leq 1/4$ (by the hypotheses: $LT^2 \leq 1/8$ and $T/h \in \mathbb{Z}$), (30) and the Cauchy-Schwarz inequality imply that

$$\sup_{s \leq T} |\tilde{V}_s(x, v)|^2 \vee \sup_{s \leq T} |\bar{v}_s(x, v)|^2 \leq 3|v|^2 + 4L^2T^2(|x|^2 + T^2|v|^2). \quad (33)$$

For all $t \geq 0$, let \mathcal{F}_t denote the sigma-algebra of events up to t generated by the independent sequence of random temporal sample points $(\mathcal{U}_i)_{i \in \mathbb{N}_0}$. Define the distorted ℓ_2 - metric⁴

$$\rho_t^2 := E|Z_t|^2 + L^{-1/2}E\langle W_t, Z_t \rangle + L^{-1}E|W_t|^2, \quad (34)$$

where $Z_t := \tilde{Q}_t(x, v) - \bar{q}_t(x, v)$ and $W_t := \tilde{V}_t(x, v) - \bar{v}_t(x, v)$. By Young's product inequality,

$$\frac{1}{2}(E|Z_t|^2 + L^{-1}E|W_t|^2) \leq \rho_t^2 \leq \frac{3}{2}(E|Z_t|^2 + L^{-1}E|W_t|^2). \quad (35)$$

⁴This type of quadratic "distorted" metric naturally arises in the study of the large-time behavior of dynamical systems with a Hamiltonian part; e.g., see (2.51) of [1]. Here we use the distorted metric differently, namely to quantify L^2 -accuracy of the sMC time integrator.

As a shorthand notation, for any $k \in \mathbb{N}_0$, let

$$\tilde{F}_{t_k} := -\nabla U(\tilde{Q}_{t_k} + (\mathcal{U}_k - t_k)\tilde{V}_{t_k}), \quad \text{and} \quad \bar{F}_{t_k} := -E[\nabla U(\bar{q}_{t_k} + (\mathcal{U}_k - t_k)\bar{v}_{t_k})].$$

Since the sMC and semi-exact flows satisfy (9) and (12) respectively,

$$Z_{t_{k+1}} = Z_{t_k} + hW_{t_k} + \frac{h^2}{2}(\tilde{F}_{t_k} - \bar{F}_{t_k}), \quad (36)$$

$$W_{t_{k+1}} = W_{t_k} + h(\tilde{F}_{t_k} - \bar{F}_{t_k}). \quad (37)$$

By the L -Lipschitz continuity of ∇U ,

$$E|\tilde{F}_{t_k} - \bar{F}_{t_k}|^2 \stackrel{\text{A.2}}{\leq} 3L^2E|Z_{t_k}|^2 + 3L^2h^2(|\tilde{V}_{t_k}|^2 + |\bar{v}_{t_k}|^2). \quad (38)$$

Moreover, since the sMC flow is an unbiased estimator of the semi-exact flow,

$$\begin{aligned} & |E[\tilde{F}_{t_k} - \bar{F}_{t_k} \mid \mathcal{F}_{t_k}]| \\ &= |E[\nabla U(\bar{q}_{t_k} + (\mathcal{U}_k - t_k)\bar{v}_{t_k}) - \nabla U(\tilde{Q}_{t_k} + (\mathcal{U}_k - t_k)\tilde{V}_{t_k}) \mid \mathcal{F}_{t_k}]|, \\ &\leq L|Z_{t_k}| + Lh|W_{t_k}|, \end{aligned} \quad (39)$$

and it follows that,

$$\begin{aligned} E\langle Z_{t_k}, \tilde{F}_{t_k} - \bar{F}_{t_k} \rangle &= E\langle Z_{t_k}, E[\tilde{F}_{t_k} - \bar{F}_{t_k} \mid \mathcal{F}_{t_k}] \rangle \stackrel{\text{A.2}}{\leq} LE[|Z_{t_k}|(|Z_{t_k}| + h|W_{t_k}|)] \\ &\leq (3/2)LE|Z_{t_k}|^2 + (1/2)Lh^2E|W_{t_k}|^2 \end{aligned} \quad (40)$$

where we used, in turn, the Cauchy-Schwarz inequality, (39), and Young's product inequality. Similarly,

$$E\langle W_{t_k}, \tilde{F}_{t_k} - \bar{F}_{t_k} \rangle \leq LE[|W_{t_k}|(|Z_{t_k}| + h|W_{t_k}|)] \quad (41)$$

$$\leq (1/2)Lh^{-1}E|Z_{t_k}|^2 + (3/2)LhE|W_{t_k}|^2. \quad (42)$$

By (36) and (37),

$$\begin{aligned} \rho_{t_{k+1}}^2 &= \text{I} + \text{II} + \text{III} \quad \text{where we have introduced} \quad (43) \\ \text{I} &:= E|Z_{t_k}|^2 + (L^{-1/2} + 2h)E\langle Z_{t_k}, W_{t_k} \rangle + (L^{-1} + L^{-1/2}h + h^2)E|W_{t_k}|^2, \\ \text{II} &:= (h^2 + L^{-1/2}h)E\langle Z_{t_k}, \tilde{F}_{t_k} - \bar{F}_{t_k} \rangle \\ &\quad + h(h^2 + \frac{3}{2}L^{-1/2}h + 2L^{-1})E\langle W_{t_k}, \tilde{F}_{t_k} - \bar{F}_{t_k} \rangle, \\ \text{III} &:= (\frac{h^4}{4} + L^{-1/2}\frac{h^3}{2} + L^{-1}h^2)E|\tilde{F}_{t_k} - \bar{F}_{t_k}|^2. \end{aligned}$$

Since $Lh^2 \leq 1/8$ implies $L^{1/2}h \leq 1/2$,

$$\begin{aligned} \text{I} &\leq (1 + 2L^{1/2}h)\rho_{t_k}^2 + (L^{1/2}h + Lh^2 - 2L^{1/2}h)L^{-1}E|W_{t_k}|^2 \\ &\leq (1 + 2L^{1/2}h)\rho_{t_k}^2 + L^{1/2}h(1 + \frac{1}{2} - 2)L^{-1}E|W_{t_k}|^2 \leq (1 + 2L^{1/2}h)\rho_{t_k}^2. \end{aligned} \quad (44)$$

By (40), (41) and (42),

$$\begin{aligned}
\Pi &\leq (h^2 + L^{-1/2}h) \left(\frac{3}{2}LE|Z_{t_k}|^2 + \frac{1}{2}Lh^2E|W_{t_k}|^2 \right) \\
&\quad + (h^2 + \frac{3}{2}L^{-1/2}h) \left(\frac{1}{2}LE|Z_{t_k}|^2 + \frac{3}{2}Lh^2E|W_{t_k}|^2 \right) + 2hL^{-1}E(W_{t_k}, \tilde{F}_{t_k} - \bar{F}_{t_k}) \\
&\leq (2Lh^2 + \frac{9}{4}L^{1/2}h)E|Z_{t_k}|^2 + (2(Lh^2)^2 + \frac{11}{4}(Lh^2)^{3/2})L^{-1}E|W_{t_k}|^2 \\
&\quad + 2hE[|W_{t_k}|(|Z_{t_k}| + h|W_{t_k}|)] \\
&\leq (2Lh^2 + \frac{9}{4}L^{1/2}h)E|Z_{t_k}|^2 + (2(Lh^2)^2 + \frac{11}{4}(Lh^2)^{3/2})L^{-1}E|W_{t_k}|^2 \\
&\quad + 2(Lh^2)L^{-1}E[|W_{t_k}|^2] + 2h \left(\frac{L^{1/2}}{2}E[|Z_{t_k}|^2] + \frac{1}{2L^{1/2}}E[|W_{t_k}|^2] \right) \\
&= \left(\frac{13}{4} + 2L^{1/2}h \right) L^{1/2}hE[|Z_{t_k}|^2] \\
&\quad + \left(2(Lh^2)^{3/2} + \frac{11}{4}Lh^2 + 2L^{1/2}h + 1 \right) (L^{1/2}h)L^{-1}E[|W_{t_k}|^2] \\
&\leq \left(\frac{13}{4} + 1 \right) L^{1/2}hE[|Z_{t_k}|^2] + \left(\frac{1}{8} + \frac{11}{32} + 2 \right) (L^{1/2}h)L^{-1}E[|W_{t_k}|^2] \\
&\leq \frac{17}{4}L^{1/2}h(E[|Z_{t_k}|^2] + L^{-1}E[|W_{t_k}|^2]) \\
&\leq \frac{17}{2}(L^{1/2}h)\rho_{t_k}^2 \tag{45}
\end{aligned}$$

where we used $L^{1/2}h \leq 1/2$, $LT^2 \leq 1/8$ and (35). Finally, by (38), and using once more $L^{1/2}h \leq 1/2$ and $Lh^2 \leq 1/8$ and (35),

$$\begin{aligned}
\Pi\text{I} &\leq \left(\frac{h^4}{4} + L^{-1/2}\frac{h^3}{2} + L^{-1}h^2 \right) (3L^2E|Z_{t_k}|^2 + 3L^2h^2(|\tilde{V}_{t_k}|^2 + |\bar{V}_{t_k}|^2)) \\
&\leq 2L^{1/2}hE|Z_{t_k}|^2 + \left(\frac{3}{4}(Lh^2)^2 + \frac{3}{2}(Lh^2)^{3/2} + 3Lh^2 \right) h^2(|\tilde{V}_{t_k}|^2 + |\bar{V}_{t_k}|^2) \\
&\leq 4L^{1/2}h\rho_{t_k}^2 + \left(\frac{3}{4}(Lh^2)^2 + \frac{3}{2}(Lh^2)^{3/2} + 3Lh^2 \right) h^2(L|x|^2 + \frac{49}{8}|v|^2) \tag{46}
\end{aligned}$$

where in the last step we inserted the a priori upper bounds from (33). Inserting (44), (45) and (46) into (43) yields

$$\rho_{t_{k+1}}^2 \leq \left(1 + \frac{29}{2}L^{1/2}h \right) \rho_{t_k}^2 + \left(\frac{3}{4}(Lh^2)^2 + \frac{3}{2}(Lh^2)^{3/2} + 3Lh^2 \right) h^2(L|x|^2 + \frac{49}{8}|v|^2).$$

By discrete Grönwall inequality in forward difference form (Lemma 15),

$$\begin{aligned}
\rho_{t_k}^2 &\leq \frac{2}{29}e^{29L^{1/2}T/2} \left(\frac{3}{4}(Lh^2)^2 + \frac{3}{2}(Lh^2)^{3/2} + 3 \right) (Lh^2)^{1/2}h^2(L|x|^2 + \frac{49}{8}|v|^2) \\
&\leq \left(\frac{6}{29} \right) \left(\frac{41}{32} \right) \left(\frac{49}{8} \right) e^{29/4} L^{1/2}h^3(L|x|^2 + |v|^2) \leq e^{31/4} L^{1/2}h^3(L|x|^2 + |v|^2).
\end{aligned}$$

Here we simplified via $LT^2 \leq 1/8$, $L^{1/2}T \leq 1/2$ and $T/h \in \mathbb{Z}$. Employing (35), and invoking the triangle inequality, gives the required upper bound. \square

Proof of Lemma 14. Define the weighted ℓ_1 -metric

$$\rho_t := |z_t| + L^{-1/2}|w_t|, \quad (47)$$

where $z_t := \bar{q}_t(x, v) - q_t(x, v)$ and $w_t := \bar{v}_t(x, v) - v_t(x, v)$. As a shorthand, let $\bar{F}_{t_k} := -E[\nabla U(\bar{q}_{t_k} + (\mathcal{U}_k - t_k)\bar{v}_{t_k})]$ and $F_t := -\nabla U(q_t)$. Since the exact and semi-exact flows satisfy (11) and (12) respectively, we have

$$z_{t_{k+1}} = z_{t_k} + hw_{t_k} + \int_{t_k}^{t_{k+1}} \int_{t_k}^s [\bar{F}_{t_k} - F_r] dr ds, \quad (48)$$

$$w_{t_{k+1}} = w_{t_k} + h\bar{F}_{t_k} - \int_{t_k}^{t_{k+1}} F_s ds. \quad (49)$$

By the triangle inequality and A.2,

$$\begin{aligned} |\bar{F}_{t_k} - F_r| &\leq |F_r - F_{t_k}| + |F_{t_k} - \bar{F}_{t_k}| = |\nabla U(q_r) - \nabla U(q_{t_k})| + |F_{t_k} - \bar{F}_{t_k}| \\ &\stackrel{\text{A.2}}{\leq} L \int_{t_k}^r v_u du + L(|z_{t_k}| + h \sup_{s \leq T} |\bar{v}_s|) \\ &\stackrel{\text{A.2}}{\leq} Lh \sup_{s \leq T} |v_s| + L(|z_{t_k}| + h \sup_{s \leq T} |\bar{v}_s|). \end{aligned} \quad (50)$$

Moreover, since the semi-exact flow incorporates the average of the potential force over each stratum,

$$\begin{aligned} &|h\bar{F}_{t_k} - \int_{t_k}^{t_{k+1}} F_s ds| \\ &\leq \left| \int_{t_k}^{t_{k+1}} \left[\nabla U(\bar{q}_{t_k} + (s - t_k)\bar{v}_{t_k}) - \nabla U(q_{t_k} + (s - t_k)v_{t_k} + \int_{t_k}^s (s - r)F_r dr) \right] ds \right| \\ &\stackrel{\text{A.2}}{\leq} L(h|z_{t_k}| + \frac{h^2}{2}|w_{t_k}| + \frac{h^3}{6} \sup_{s \leq T} |\nabla U(q_s)|) \\ &\stackrel{\text{A.2}}{\leq} L \left(h|z_{t_k}| + \frac{h^2}{2}|w_{t_k}| + \frac{h^3}{6} (L|x| + LT \sup_{s \leq T} |v_s|) \right), \end{aligned} \quad (51)$$

where in the last step we used

$$\begin{aligned} \sup_{s \leq T} |\nabla U(q_s)| &= \sup_{s \leq T} |\nabla U(x) + \nabla U(q_s) - \nabla U(x)| \\ &\stackrel{\text{A.2}}{\leq} L|x| + L \left| \int_0^s v_u du \right| \leq L|x| + LT \sup_{s \leq T} |v_s|. \end{aligned}$$

Inserting (50) and (51) into (48) and (49) respectively, yields

$$|z_{t_{k+1}}| \leq (1 + \frac{1}{2}Lh^2)|z_{t_k}| + h|w_{t_k}| + Lh^3(\sup_{s \leq T} |v_s| \vee \sup_{s \leq T} |\bar{v}_s|), \quad (52)$$

$$|w_{t_{k+1}}| \leq (1 + \frac{1}{2}Lh^2)|w_{t_k}| + Lh|z_{t_k}| + \frac{1}{6}L^2h^3(|x| + T \sup_{s \leq T} |v_s|). \quad (53)$$

Inserting (52) and (53) into (47), and using $L^{1/2}h \leq 1/2$ (by the hypotheses: $LT^2 \leq 1/8$ and $T/h \in \mathbb{Z}$), gives

$$\begin{aligned} \rho_{t_{k+1}} &\leq \left(1 + \frac{5}{4}L^{1/2}h\right)\rho_{t_k} + \frac{1}{6}(L^{1/2}h)^3|x| \\ &\quad + (L^{1/2}h)^3\left(L^{-1/2} + \frac{1}{6}T\right)\left(\sup_{s \leq T}|v_s| \vee \sup_{s \leq T}|\bar{v}_s|\right). \end{aligned}$$

By the discrete Grönwall's inequality in forward difference form (Lemma 15),

$$\begin{aligned} \rho_{t_k} &\leq (4/5)e^{(5/4)L^{1/2}T} \left(\frac{1}{6}(L^{1/2}h)^2|x| + (L^{1/2}h)^2\left(L^{-1/2} + \frac{1}{6}T\right)\left(\sup_{s \leq T}|v_s| \vee \sup_{s \leq T}|\bar{v}_s|\right) \right) \\ &\leq (4/5)e^{5/8}L^{1/2}h^2 \left(\frac{1}{6}L^{1/2}|x| + \left(1 + \frac{1}{6}L^{1/2}T\right)\left(\sup_{s \leq T}|v_s| \vee \sup_{s \leq T}|\bar{v}_s|\right) \right) \\ &\leq (4/5)e^{5/8}L^{1/2}h^2 \left(\frac{1}{6}L^{1/2}|x| + \left(\frac{13}{12}\right)\left(\frac{5}{8}L^{1/2}|x| + \frac{37}{32}|v|\right) \right) \\ &\leq (4/5)e^{5/8}L^{1/2}h^2 \left(\frac{27}{32}L^{1/2}|x| + \frac{481}{384}|v| \right) \leq 2e^{5/8}L^{1/2}(L^{1/2}|x| + |v|)h^2, \end{aligned}$$

which gives (32) — as required. Note that in the last two steps we inserted the *a priori* upper bound in (30) and applied the conditions $LT^2 \leq 1/8$ and $L^{1/2}h \leq 1/2$. \square

3. Duration-Randomized uHMC with sMC Time Integration

Here we consider a duration-randomized uHMC algorithm with complete velocity refreshment (or *randomized uHMC* for short). In order to avoid periodicities in the Hamiltonian steps of HMC, duration randomization was suggested by Mackenzie in 1989 [30]. There are a number of ways to incorporate duration randomization into uHMC [9, 36, 7, 4] including randomizing the time step and/or randomizing the # of integration steps. One overlooked way, which is perhaps the simplest to analyze, is the unadjusted (or inexact) Markov jump process on phase space introduced in [7, Section 6], as briefly recounted below.

Before delving into more detail, it is worthwhile to remark that duration randomization has a similar effect as non-randomized uHMC with partial velocity refreshment. Intuitively speaking, after a random # of non-randomized uHMC transition steps with partial velocity refreshment, a complete velocity refreshment occurs. Therefore, the findings given below are expected to hold for non-randomized uHMC with partial velocity refreshment. However, in comparison to randomized uHMC, the analysis of non-randomized uHMC with partial velocity refreshment is a more demanding task if the bounds have to be realistic with respect to model and hyper parameters.

3.1. Definition of Randomized uHMC with sMC time integration

The randomized uHMC process is an implementable, inexact MCMC method defined on *phase space* \mathbb{R}^{2d} and aimed at the Boltzmann-Gibbs distribution

$$\mu_{BG} := \mu \otimes \mathcal{N}(0, I_d) . \quad (54)$$

First, we define the infinitesimal generator of the randomized uHMC process; and then describe how a path of this process can be realized.

To define the infinitesimal generator, let $\mathcal{U} \sim \text{Uniform}(0, h)$ and $\xi \sim \mathcal{N}(0, I_d)$ be independent random variables. Denote by $\Theta_h(x, v, \mathcal{U})$ a single step of the sMC time integrator operated with time step size $h > 0$ and initial condition $(x, v) \in \mathbb{R}^{2d}$ where $\Theta_h : \mathbb{R}^{2d} \times (0, 1) \rightarrow \mathbb{R}^{2d}$ is the deterministic map defined by

$$\Theta_h : (x, v, u) \mapsto \left(x + hv + \frac{h^2}{2} F(x + uv), v + hF(x + uv) \right) . \quad (55)$$

Recall that $F \equiv -\nabla U$. On functions $f : \mathbb{R}^{2d} \rightarrow \mathbb{R}^{2d}$, the infinitesimal generator of the randomized uHMC process is defined by

$$\tilde{\mathcal{G}}f(x, v) = h^{-1} E (f(\Theta_h(x, v, \mathcal{U})) - f(x, v)) + \lambda E (f(x, \xi) - f(x, v)) , \quad (56)$$

where $\lambda > 0$ is the intensity of velocity randomizations and $h > 0$ is the step size. The operator $\tilde{\mathcal{G}}$ is the generator of a Markov jump process $(\tilde{Q}_t, \tilde{V}_t)_{t \geq 0}$ with jumps that result in either: (i) a step of the sMC time integrator Θ_h ; or (ii) a complete velocity randomization $(x, v) \mapsto (x, \xi)$. As we will see below, due to time-discretization error in the sMC steps, this process has an asymptotic bias. Since the number of jumps of the process over $[0, t]$ is a Poisson process with intensity $\lambda + h^{-1}$, the mean number of steps of Θ_h (and hence, gradient evaluations) over a time interval of length $t > 0$ is t/h .

The random jump times and embedded chain of the randomized uHMC process may be produced by iterating the following algorithm.

Algorithm (Randomized uHMC). *Given intensity $\lambda > 0$, step size $h > 0$, the current time T_0 , and the current state $(\tilde{Q}_{T_0}, \tilde{V}_{T_0}) \in \mathbb{R}^{2d}$, the method outputs an updated state $(\tilde{Q}_{T_1}, \tilde{V}_{T_1}) \in \mathbb{R}^{2d}$ at the random time T_1 using the following steps.*

Step 1 *Draw an exponential random variable ΔT with mean $h/(\lambda h + 1)$, and update time via $T_1 = T_0 + \Delta T$.*

Step 2 *Draw $\xi \sim \mathcal{N}(0, I_d)$, $\mathcal{U} \sim \text{Uniform}(0, h)$, $\mathcal{V} \sim \text{Uniform}(0, 1)$, and set*

$$(\tilde{Q}_{T_1}, \tilde{V}_{T_1}) = \begin{cases} (\tilde{Q}_{T_0}, \xi) & \mathcal{V} \leq \frac{\lambda h}{1 + \lambda h} \\ \Theta_h(\tilde{Q}_{T_0}, \tilde{V}_{T_0}, \mathcal{U}) & \text{otherwise} . \end{cases}$$

Note: the random variables ΔT , ξ , \mathcal{V} , and \mathcal{U} are mutually independent and independent of the state of the process.

Let $\{T_i\}_{i \in \mathbb{N}_0}$ and $\{(\tilde{Q}_{T_i}, \tilde{V}_{T_i})\}_{i \in \mathbb{N}_0}$ denote the sequence of random jump times and states obtained by iterating this algorithm. The path of the randomized uHMC process is then given by

$$(Q_t, V_t) = (\tilde{Q}_{T_i}, \tilde{V}_{T_i}) \quad \text{for } t \in [T_i, T_{i+1}).$$

Moreover, for any $t > 0$, the time-average of an observable $f : \mathbb{R}^{2d} \rightarrow \mathbb{R}$ along this trajectory is given by:

$$\frac{1}{t} \int_0^t f(Q_s, V_s) ds = \frac{1}{t} \sum_{0 \leq i \leq \infty} f(Q_{T_i}, V_{T_i}) (t \wedge T_{i+1} - t \wedge T_i).$$

Let $\theta_h : \mathbb{R}^{2d} \times (0, 1) \rightarrow \mathbb{R}^{2d}$ denote the map that advances the exact solution of the Hamiltonian dynamics over a single time step of size $h > 0$, i.e.,

$$\theta_h : (x, v) \mapsto \left(x + hv + \int_0^h (h-s) F(q_s(x, v)), v + \int_0^h F(q_s(x, v)) ds \right).$$

In the asymptotic bias proof, we couple the randomized uHMC process to a corresponding *exact* process $(Q_t, V_t)_{t \geq 0}$ with generator defined by:

$$\mathcal{G}f(x, v) = h^{-1} E(f(\theta_h(x, v)) - f(x, v)) + \lambda E(f(x, \xi) - f(x, v)). \quad (57)$$

A key property of the exact process is that it leaves infinitesimally invariant the Boltzmann-Gibbs distribution μ_{BG} , and under our regularity assumptions on the target measure μ , it can be verified that μ_{BG} is also the unique invariant measure of the exact process.

3.2. L^2 -Wasserstein Contractivity of Randomized uHMC

Let $(\tilde{p}_t)_{t \geq 0}$ denote the transition semigroup of the randomized uHMC process $((\tilde{Q}_t, \tilde{V}_t))_{t \geq 0}$. A key tool in the contraction proof is a coupling of two copies of the randomized uHMC process with generator defined by

$$\begin{aligned} \tilde{\mathcal{G}}^C f(y) &= h^{-1} E(f(\Theta_h(x, v, \mathcal{U}), \Theta_h(\tilde{x}, \tilde{v}, \mathcal{U})) - f(y)) \\ &\quad + \lambda E(f((x, \xi), (\tilde{x}, \xi)) - f(y)) \end{aligned} \quad (58)$$

where $y = ((x, v), (\tilde{x}, \tilde{v})) \in \mathbb{R}^{4d}$.

To measure the distance between the two copies we use a distorted metric:

$$\begin{aligned} \rho(y)^2 &:= \frac{1}{4} |z|^2 + \frac{\lambda^{-1}}{2} \langle z, w \rangle + \lambda^{-2} |w|^2 = \begin{pmatrix} z & w \end{pmatrix} \mathbf{A} \begin{pmatrix} z \\ w \end{pmatrix}, \quad \text{where} \\ y &= ((x, v), (\tilde{x}, \tilde{v})) \in \mathbb{R}^{4d}, \quad z := x - \tilde{x}, \quad w := v - \tilde{v}, \quad \mathbf{A} := \begin{bmatrix} \frac{1}{4} \mathbf{1}_d & \frac{\lambda^{-1}}{4} \mathbf{1}_d \\ \frac{\lambda^{-1}}{4} \mathbf{1}_d & \lambda^{-2} \mathbf{1}_d \end{bmatrix}. \end{aligned} \quad (59)$$

This distorted metric involves the “ qv trick” behind Foster-Lyapunov functions for (i) dissipative Hamiltonian systems with random impulses [38]; (ii) second-order Langevin processes [32, 40, 1]; and (iii) exact randomized HMC [7]. This

cross-term plays a crucial role since it captures the contractivity of the potential force. Using the Peter-Paul inequality with parameter δ , we can compare this distorted metric to a ‘straightened’ metric,

$$\rho(y)^2 \leq \left(\frac{1}{4} + \frac{\lambda^{-1}\delta}{4} \right) |z|^2 + \left(\lambda^{-2} + \frac{\lambda^{-1}}{4\delta} \right) |w|^2 \stackrel{\delta=3\lambda}{\leq} |z|^2 + \frac{13}{12} \lambda^{-2} |w|^2 \quad (60)$$

$$\leq \max(K^{-1}, \frac{13}{12} \lambda^{-2}) (K|z|^2 + |w|^2) . \quad (61)$$

Similarly, the distorted metric is equivalent to the standard Euclidean metric

$$\frac{1}{8} \min(1, 4\lambda^{-2}) (|z|^2 + |w|^2) \leq \rho(y)^2 \leq \max(1, \frac{13}{12} \lambda^{-2}) (|z|^2 + |w|^2) . \quad (62)$$

By applying the generator $\tilde{\mathcal{G}}^C$ on this distorted metric, and using the co-coercivity property of ∇U (see Remark 4), we can prove the following.

Lemma 16. *Suppose that Assumptions A.1-A.3 hold and $\lambda > 0$, $h > 0$ satisfy*

$$(L\lambda^{-2})^{1/2} \leq 12^{-1} , \quad (63)$$

$$\lambda h \leq 1 . \quad (64)$$

Then $\tilde{\mathcal{G}}^C$ satisfies the following infinitesimal contractivity result

$$\tilde{\mathcal{G}}^C \rho^2 \leq -\gamma \rho^2 , \quad \text{where } \gamma := 10^{-1} \frac{K}{\lambda} . \quad (65)$$

The proof of Lemma 16 is deferred to Section 3.4. As a consequence of Lemma 16, we can prove L^2 Wasserstein contractivity of the transition semigroup $(\tilde{p}_t)_{t \geq 0}$ of randomized uHMC.

Theorem 17. *Suppose that Assumptions A.1-A.3 hold and $\lambda > 0$, $h > 0$ satisfy (63) and (64), respectively. Then for any pair of probability measures $\nu, \eta \in \mathcal{P}^2(\mathbb{R}^{2d})$, and for any $t \geq 0$,*

$$\mathcal{W}^2(\nu \tilde{p}_t, \eta \tilde{p}_t) \leq 3 \max(\lambda, \lambda^{-1}) e^{-\gamma t/2} \mathcal{W}^2(\nu, \eta) . \quad (66)$$

Proof of Theorem 17. Let $(Y_t)_{t \geq 0}$ denote the coupling process on \mathbb{R}^{4d} generated by $\tilde{\mathcal{G}}^C$ with initial distribution given by an optimal coupling of the initial distributions ν and η w.r.t. the distance \mathcal{W}^2 . As a consequence of Lemma 16, the process $t \mapsto e^{\gamma t} \rho(Y_t)^2$ is a non-negative supermartingale. Moreover, by using the equivalence to the standard Euclidean metric given in (62),

$$\begin{aligned} \mathcal{W}^2(\nu \tilde{p}_t, \eta \tilde{p}_t)^2 &\leq 8 \max(1, \frac{1}{4} \lambda^2) E[\rho(Y_t)^2] \stackrel{(65)}{\leq} 8 \max(1, \frac{1}{4} \lambda^2) e^{-\gamma t} E[\rho(Y_0)^2] \\ &\leq 8 \max(1, \frac{1}{4} \lambda^2) \max(1, \frac{13}{12} \lambda^{-2}) e^{-\gamma t} \mathcal{W}^2(\nu, \eta)^2 \\ &\leq 9 \max(\lambda^2, \lambda^{-2}) e^{-\gamma t} \mathcal{W}^2(\nu, \eta)^2 . \end{aligned}$$

Taking square roots of both sides gives the required result. \square

3.3. L^2 -Wasserstein Asymptotic Bias of Randomized uHMC

As a consequence of Theorem 17, the randomized uHMC process admits a unique invariant measure denoted by $\tilde{\mu}_{BG}$. Here we quantify the L^2 -Wasserstein asymptotic bias, i.e., $\mathcal{W}^2(\mu_{BG}, \tilde{\mu}_{BG})$. A key tool in the asymptotic bias proof is a coupling of the unadjusted and exact processes with generator

$$\begin{aligned} \mathcal{A}^C f(y) &= h^{-1} E(f(\theta_h(x, v), \Theta_h(\tilde{x}, \tilde{v}, \mathcal{U})) - f(y)) \\ &\quad + \lambda E(f((x, \xi), (\tilde{x}, \xi)) - f(y)) , \end{aligned} \quad (67)$$

where $y = ((x, v), (\tilde{x}, \tilde{v})) \in \mathbb{R}^{4d}$.

Lemma 18. *Suppose that Assumptions A.1-A.3 hold and $\lambda > 0$ and $h > 0$ satisfy (63) and (64), respectively. Let γ be the contraction rate of randomized uHMC in (65). Then \mathcal{A}^C satisfies the following infinitesimal drift condition*

$$\mathcal{A}^C \rho(y)^2 \leq -\frac{\gamma}{2} \rho(y)^2 + \frac{1}{2} \left(1 + \frac{1}{K\lambda^{-2}}\right) (L^{3/2}h|x|^2 + |v|^2) L h^3 , \quad (68)$$

for all $y = ((x, v), (\tilde{x}, \tilde{v})) \in \mathbb{R}^{4d}$.

The proof of Lemma 18 is deferred to Section 3.4. Let $(p_t)_{t \geq 0}$ denote the transition semigroup of the exact process $((Q_t, V_t))_{t \geq 0}$. We are now in position to quantify the asymptotic bias of randomized uHMC with sMC time integration.

Theorem 19. *Suppose that Assumptions A.1-A.3 hold and $\lambda > 0$ and $h > 0$ satisfy (63) and (64), respectively. Then*

$$\mathcal{W}^2(\mu, \tilde{\mu})^2 \leq 8\gamma^{-1} \left(1 + \frac{\lambda^2}{K}\right) L (L^{3/2}K^{-1}h^4d + h^3d) . \quad (69)$$

Remark 20 (Why duration randomization?). *Since the number of jumps of the randomized uHMC process over $[0, t]$ is a Poisson process with intensity $\lambda + h^{-1}$, the mean number of steps of Θ_h (and hence, gradient evaluations) over a time interval of length t is t/h . Let ν be the initial distribution of the randomized uHMC process. We choose λ to saturate (63), i.e., $\lambda = 12L^{1/2}$. The contraction rate in (65) then becomes*

$$\gamma = 120^{-1} K^{1/2} \left(\frac{K}{L}\right)^{1/2} .$$

According to Theorem 17, to obtain ε -accuracy in \mathcal{W}^2 w.r.t. $\tilde{\mu}$, t can be chosen such that

$$t = 240K^{-1/2} \left(\frac{L}{K}\right)^{1/2} \log \left(\frac{3 \max(12^{-1}L^{1/2}, 12L^{-1/2}) \mathcal{W}^2(\nu, \tilde{\mu}_{BG})}{\varepsilon} \right)^+ . \quad (70)$$

However, since $\tilde{\mu}$ is inexact, to resolve the asymptotic bias to ε -accuracy in \mathcal{W}^2 , Theorem 19 indicates that it suffices to choose h such that

$$8 \cdot 120 \cdot \left(Kd \left(\frac{L}{K}\right)^4 h^4 + K^{1/2}d \left(\frac{L}{K}\right)^{5/2} h^3 \right) \leq \varepsilon^2 .$$

In other words, it suffices to choose h such that

$$h^{-1} \geq 2 \max \left((60)^{1/4} K^{1/2} \left(\frac{d}{K} \right)^{1/4} \frac{L}{K} \varepsilon^{-1/2}, 2(15)^{1/3} K^{1/2} \left(\frac{d}{K} \right)^{1/3} \left(\frac{L}{K} \right)^{5/6} \varepsilon^{-2/3} \right). \quad (71)$$

Combining (70) and (71) gives an overall complexity of

$$\begin{aligned} \frac{t}{h} \propto \max & \left(\left(\frac{d}{K} \right)^{1/4} \left(\frac{L}{K} \right)^{3/2} \varepsilon^{-1/2}, \left(\frac{d}{K} \right)^{1/3} \left(\frac{L}{K} \right)^{4/3} \varepsilon^{-2/3} \right) \\ & \times \log \left(\frac{\max(L^{1/2}, L^{-1/2}) \mathcal{W}^2(\nu, \tilde{\mu}_{BG})}{\varepsilon} \right)^+. \end{aligned} \quad (72)$$

Proof of Theorem 19. Let $(Y_t)_{t \geq 0}$ be the coupling process generated by \mathcal{A}^C in (67) with initial condition $Y_0 = ((Q_0, V_0), (\tilde{Q}_0, \tilde{V}_0)) \sim \mu_{BG} \otimes \tilde{\mu}_{BG}$. Fix $t > 0$. Then by the coupling characterization of the L^2 -Wasserstein distance, and Itô's formula for jump processes applied to $t \mapsto e^{\gamma t/2} \Phi(Y_t)$, we obtain

$$\begin{aligned} \mathcal{W}^2(\mu, \tilde{\mu})^2 & \leq E(|Q_0 - \tilde{Q}_0|^2) \leq \frac{16}{3} E \left(\frac{3}{16} |Q_0 - \tilde{Q}_0|^2 + \lambda^{-2} \left| V_0 - \tilde{V}_0 + \frac{\lambda}{4} (Q_0 - \tilde{Q}_0) \right|^2 \right) \\ & \leq \frac{16}{3} E \rho(Y_0)^2 = \frac{16}{3} E \rho(Y_t)^2 \\ & \leq \frac{16}{3} \left(e^{-\gamma t/2} E \rho(Y_0)^2 + \int_0^t e^{-\gamma(t-s)/2} \left(\frac{\gamma}{2} \rho(Y_s)^2 + \mathcal{A}^C \rho(Y_s)^2 \right) ds \right) \\ & \stackrel{\text{Lem. 18}}{\leq} 8e^{-\gamma t/2} E \rho(Y_0)^2 \\ & \quad + 4 \left(1 + \frac{1}{K\lambda^{-2}} \right) L h^3 \int_0^t e^{-\gamma(t-s)/2} (L^{3/2} h E |Q_s|^2 + E |V_s|^2) ds. \end{aligned}$$

Since the exact process leaves μ_{BG} invariant, the integrand in this expression simplifies

$$\begin{aligned} \mathcal{W}^2(\mu, \tilde{\mu})^2 & \leq 8e^{-\gamma t/2} E \rho(Y_0)^2 \\ & \quad + 4 \left(1 + \frac{1}{K\lambda^{-2}} \right) L h^3 (L^{3/2} h E |Q_0|^2 + d) \int_0^t e^{-\gamma(t-s)/2} ds \\ & \stackrel{\text{Rem. 3}}{\leq} 8\gamma^{-1} \left(1 + \frac{\lambda^2}{K} \right) \frac{L}{K} h^3 d (L^{3/2} h + K). \end{aligned}$$

Simplifying this expression gives (69). \square

3.4. Proofs for Randomized uHMC

Proof of Lemma 16. Let $F_U := F(x + Uv)$, $\tilde{F}_U := F(\tilde{x} + U\tilde{v})$, $Z_U := z + Uw$, and $\Delta F_U := F_U - \tilde{F}_U$. Note that by A.2, A.3 and (13),

$$K |Z_U|^2 \stackrel{\text{A.3}}{\leq} -\langle Z_U, \Delta F_U \rangle \stackrel{\text{A.2}}{\leq} L |Z_U|^2, \quad |\Delta F_U|^2 \stackrel{(13)}{\leq} -L \langle Z_U, \Delta F_U \rangle. \quad (73)$$

The idea of this proof is to decompose $\tilde{\mathcal{G}}^C \rho(y)^2$ into a gain Γ_0 and loss Λ_0 , and use (73) and the hyperparameter assumptions, to obtain an overall gain.

To this end, evaluate (58) at $f(y) = \rho(y)^2$ to obtain,

$$\begin{aligned} \tilde{\mathcal{G}}^C \rho(y)^2 &= h^{-1} E \left(\rho(\Theta_h(x, v, \mathcal{U}), \Theta_h(\tilde{x}, \tilde{v}, \mathcal{U}))^2 - \rho(y)^2 \right) \\ &\quad + \lambda E \left(\rho((x, \xi), (\tilde{x}, \xi))^2 - \rho(y)^2 \right) \\ &= \lambda^{-1} \left(\frac{\lambda h}{4} + \frac{1}{2} \right) E \langle Z_{\mathcal{U}}, \Delta F_{\mathcal{U}} \rangle + \lambda^{-1} \left(-\frac{1}{2} + \frac{\lambda h}{4} \right) |w|^2 \\ &\quad + \lambda^{-1} E \left[\left(\frac{\lambda^2 h^2}{4} + \frac{3\lambda h}{4} + 2 - \lambda \mathcal{U} \left(\frac{\lambda h}{4} + \frac{1}{2} \right) \right) \lambda^{-1} \langle w, \Delta F_{\mathcal{U}} \rangle \right] \\ &\quad + \lambda^{-1} \left(\frac{\lambda^3 h^3}{16} + \frac{\lambda^2 h^2}{4} + \lambda h \right) \lambda^{-2} E |\Delta F_{\mathcal{U}}|^2 = \Gamma_0 + \Lambda_0 \quad \text{where} \\ \Gamma_0 &:= \lambda^{-1} \left(\frac{\lambda h}{4} + \frac{1}{2} \right) E \langle Z_{\mathcal{U}}, \Delta F_{\mathcal{U}} \rangle - \lambda^{-1} \frac{1}{2} |w|^2 \end{aligned} \quad (74)$$

$$\begin{aligned} \Lambda_0 &:= \lambda^{-1} \left(\frac{\lambda^3 h^3}{16} + \frac{\lambda^2 h^2}{4} + \lambda h \right) \lambda^{-2} E |\Delta F_{\mathcal{U}}|^2 + \lambda^{-1} \left(\frac{\lambda h}{4} \right) |w|^2 \\ &\quad + \lambda^{-1} E \left[\left(\frac{\lambda^2 h^2}{4} + \frac{3\lambda h}{4} + 2 - \lambda \mathcal{U} \left(\frac{\lambda h}{4} + \frac{1}{2} \right) \right) \lambda^{-1} \langle w, \Delta F_{\mathcal{U}} \rangle \right]. \end{aligned} \quad (75)$$

Note that the term $\lambda^{-1} E \left[\lambda \mathcal{U} \left(\frac{\lambda h}{4} + \frac{1}{2} \right) \lambda^{-1} \langle w, \Delta F_{\mathcal{U}} \rangle \right]$ was added and subtracted in order to leverage the co-coercivity property of ∇U at $Z_{\mathcal{U}}$; see (73). By the Peter-Paul inequality with parameter $(L\lambda^{-2})^{1/2}$, $\lambda h \leq 1$, and (73),

$$\begin{aligned} \Lambda_0 &\leq \lambda^{-1} \left(\frac{\lambda^3 h^3}{16} + \frac{\lambda^2 h^2}{4} + \lambda h + \frac{1}{2(L\lambda^{-2})^{1/2}} \left(\frac{\lambda^2 h^2}{4} + \frac{3\lambda h}{4} + 2 \right) \right) \lambda^{-2} E |\Delta F_{\mathcal{U}}|^2 \\ &\quad + \lambda^{-1} \left(\frac{\lambda h}{4} + \frac{(L\lambda^{-2})^{1/2}}{2} \left(\frac{\lambda^2 h^2}{4} + \frac{3\lambda h}{4} + 2 \right) \right) |w|^2 \\ &\stackrel{(64)}{\leq} \lambda^{-1} \left(\frac{21}{16} + \frac{3}{2(L\lambda^{-2})^{1/2}} \right) \lambda^{-2} E |\Delta F_{\mathcal{U}}|^2 + \lambda^{-1} \left(\frac{1}{4} + \frac{3(L\lambda^{-2})^{1/2}}{2} \right) |w|^2 \\ &\stackrel{(73)}{\leq} -\lambda^{-1} \left(\frac{21L\lambda^{-2}}{16} + \frac{3(L\lambda^{-2})^{1/2}}{2} \right) E \langle Z_{\mathcal{U}}, \Delta F_{\mathcal{U}} \rangle + \lambda^{-1} \left(\frac{1}{4} + \frac{3(L\lambda^{-2})^{1/2}}{2} \right) |w|^2 \\ &\stackrel{(63)}{\leq} -\lambda^{-1} \left(\frac{21}{16 \cdot 12^2} + \frac{1}{8} \right) E \langle Z_{\mathcal{U}}, \Delta F_{\mathcal{U}} \rangle + \lambda^{-1} \frac{3}{8} |w|^2. \end{aligned} \quad (76)$$

Combining Γ_0 in (74) with the upper bound on Λ_0 in (76) yields an overall gain

$$\tilde{\mathcal{G}}^C \rho(y)^2 \leq -\frac{1}{8} \lambda^{-1} \left(-E \langle Z_{\mathcal{U}}, \Delta F_{\mathcal{U}} \rangle + |w|^2 \right) \stackrel{(73)}{\leq} -\frac{1}{8} \lambda^{-1} \left(KE |Z_{\mathcal{U}}|^2 + |w|^2 \right).$$

By the Peter-Paul inequality with parameter h and noting that $\mathcal{U} \sim$

Uniform(0, h),

$$\begin{aligned}\tilde{\mathcal{G}}^C \rho(y)^2 &\leq -\frac{1}{8}\lambda^{-1} \left(\frac{5}{2}K(|z|^2 + h\langle z, w \rangle + \frac{h^2}{3}|w|^2) + |w|^2 \right) \\ &\leq -\frac{1}{8}\lambda^{-1} \left(\frac{5}{4}K|z|^2 + \left(1 - \frac{5}{12}Kh^2\right)|w|^2 \right) \stackrel{(63)}{\leq} -\frac{1}{9}\lambda^{-1} (K|z|^2 + |w|^2),\end{aligned}$$

where in the last step we used $K \leq L$, $\lambda h \leq 1$ and $(L\lambda^{-2})^{1/2} \leq 12^{-1}$. Inserting (61) and simplifying yields the required infinitesimal contraction result, i.e.,

$$\tilde{\mathcal{G}}^C \rho(y)^2 \leq -\frac{1}{9}\lambda^{-1} \min\left(\frac{12}{13}\lambda^2, K\right)\rho(y)^2 \leq -\frac{1}{10} \min(\lambda, K\lambda^{-1})\rho(y)^2 = -\frac{K}{10\lambda}\rho(y)^2,$$

since $K\lambda^{-2} \leq 12^{-1} < 1$ implies $K < \lambda^2$, and hence, $\min(\lambda, K\lambda^{-1}) = K\lambda^{-1}$. \square

Proof of Lemma 18. Let $F_{\mathcal{U}} := F(x + \mathcal{U}v)$, $\tilde{F}_{\mathcal{U}} := F(\tilde{x} + \mathcal{U}\tilde{v})$, $Z_{\mathcal{U}} := z + \mathcal{U}w$, and $\Delta F_{\mathcal{U}} := F_{\mathcal{U}} - \tilde{F}_{\mathcal{U}}$. The idea of this proof is related to the proof of Lemma 16: we carefully decompose $\mathcal{A}^C \rho(y)^2$ into a gain Γ , loss Λ , and also, a discretization error Δ , and use (73) and the hyperparameter assumptions, to obtain a gain from the contractivity of the underlying randomized uHMC process up to discretization error. This estimate results in an infinitesimal drift condition, as opposed to an infinitesimal contractivity result. The quantification of the discretization error is related to the L^2 -error estimates for the sMC time integrator developed in Lemma 7, though the semi-exact flow only implicitly appears below, since the proof involves a one step analysis.

As a preliminary step, we develop some estimates that are used to bound the discretization error. Recall that $(q_s(x, v), v_s(x, v))$ denotes the exact Hamiltonian flow. Since $Lh^2 \leq 12^{-2} \leq 1/4$ (by the hypotheses: $(L\lambda^{-2})^{1/2} \leq 1/12$ and $\lambda h \leq 1$), (30) and the Cauchy-Schwarz inequality imply that

$$\sup_{s \leq h} |v_s(x, v)|^2 \leq 3|v|^2 + 4L^2h^2(|x|^2 + h^2|v|^2) \leq 4L^2h^2|x|^2 + \frac{31}{10}|v|^2. \quad (77)$$

As a shorthand, define

$$\begin{aligned}F_1 &:= \frac{2}{h^2} \int_0^h (h-s)F(q_s(x, v))ds, \quad \Delta F_1 := \frac{2}{h^2} \int_0^h (h-s)[F(q_s(x, v)) - F_{\mathcal{U}}]ds, \\ F_2 &:= \frac{1}{h} \int_0^h F(q_s(x, v))ds, \quad \text{and} \quad \Delta F_2 := \frac{1}{h} \int_0^h [F(q_s(x, v)) - F_{\mathcal{U}}]ds.\end{aligned}$$

Then by the Cauchy-Schwarz inequality

$$\begin{aligned}E|\Delta F_1|^2 &= E \left| \frac{2}{h^2} \int_0^h (h-s)[F(q_s) - F_{\mathcal{U}}]ds \right|^2 \leq \frac{4}{h^4} \frac{h^3}{3} \int_0^h E|F(q_s) - F_{\mathcal{U}}|^2 ds \\ &\stackrel{\text{A.2}}{\leq} \frac{4}{h^4} \frac{L^2h^3}{3} \int_0^h E|q_s - x - \mathcal{U}v|^2 ds = \frac{4}{h^4} \frac{L^2h^3}{3} \int_0^h E \left| \int_0^s v_r dr - \mathcal{U}v \right|^2 ds \\ &\leq \frac{4}{h^4} \frac{2L^2h^3}{3} \left(\int_0^h \left| \int_0^s v_r dr \right|^2 ds + h^3|v|^2 \right) \leq \frac{8L^2h^2}{3} \left(\sup_{s \leq h} |v_s|^2 + |v|^2 \right) \\ &\stackrel{(77)}{\leq} \frac{8L^2h^2}{3} \left(4L^2h^2|x|^2 + \frac{41}{10}|v|^2 \right) \quad (78)\end{aligned}$$

where in the next to last step we used Young's product inequality. Similarly,

$$\begin{aligned}
 E|\Delta F_2|^2 &= E \left| \frac{1}{h} \int_0^h [F(q_s(x, v)) - F_{\mathcal{U}}] ds \right|^2 \leq h^{-1} E \int_0^h |F(q_s(x, v)) - F_{\mathcal{U}}|^2 ds \\
 &\stackrel{\text{A.2}}{\leq} \frac{L^2}{h} \int_0^h E \left| \int_0^s v_r dr - \mathcal{U}v \right|^2 ds \leq \frac{2L^2}{h} \left(\int_0^h \left| \int_0^s v_r dr \right|^2 ds + h^3 |v|^2 \right) \\
 &\leq 2L^2 h^2 \left(\sup_{s \leq h} |v_s|^2 + |v|^2 \right) \stackrel{(77)}{\leq} 2L^2 h^2 \left(4L^2 h^2 |x|^2 + \frac{41}{10} |v|^2 \right). \quad (79)
 \end{aligned}$$

Combining (78) and (79) we obtain

$$E|\Delta F_1|^2 \vee E|\Delta F_2|^2 \leq \frac{8}{3} L^2 h^2 \left(4L^2 h^2 |x|^2 + \frac{41}{10} |v|^2 \right) \leq 11L^2 h^2 (L^2 h^2 |x|^2 + |v|^2). \quad (80)$$

In order to obtain a sharp error estimate for the sMC time integrator, the following upper bound is crucial

$$\begin{aligned}
 |E\Delta F_2| &= \left| \frac{1}{h} E \int_0^h [F(q_s(x, v)) - F_{\mathcal{U}}] ds \right| = \left| \frac{1}{h} \int_0^h [F(q_s(x, v)) - F(x + sv)] ds \right| \\
 &\stackrel{\text{A.2}}{\leq} \frac{L}{h} \int_0^h |q_s(x, v) - (x + sv)| ds \leq \frac{L}{h} \int_0^h \left| \int_0^s (s-r) F(q_r(x, v)) dr \right| ds \\
 &\stackrel{\text{A.2}}{\leq} \frac{L}{h} \int_0^h \int_0^s (s-r) |F(q_r(x, v))| dr ds \leq \frac{L^2 h^2}{6} (|x| + h \sup_{s \leq h} |v_s|) \\
 &\stackrel{(30)}{\leq} \frac{L^2 h^2}{6} (|x| + h[|v| + Lh(1 + Lh^2)](|x| + h|v|)) \stackrel{(63)}{\leq} \frac{L^2 h^2}{5} (|x| + h|v|).
 \end{aligned}$$

Thus, by Cauchy-Schwarz inequality,

$$|E\Delta F_2|^2 \leq \frac{2L^4 h^4}{25} (|x|^2 + h^2 |v|^2) \stackrel{(63)}{\leq} \frac{L^3 h^4}{12} (L|x|^2 + |v|^2), \quad (81)$$

in the last step the numerical pre-factor was simplified by using $\lambda h \leq 1$ and $(L\lambda^{-2})^{1/2} \leq 12^{-1}$.

Evaluate (67) at $f(y) = \rho(y)^2$ and expand to obtain

$$\begin{aligned}
\mathcal{A}^C \rho(y)^2 &= h^{-1} E(\rho(\theta_h(x, v), \Theta_h(\tilde{x}, \tilde{v}, \mathcal{U}))^2 - \rho(y)^2) \\
&\quad + \lambda E(\rho((x, \xi), (\tilde{x}, \xi))^2 - \rho(y)^2) \\
&= \lambda^{-1} \frac{1}{2} E\langle z, F_2 - \tilde{F}_U \rangle + \lambda^{-1} \frac{\lambda h}{4} E\langle z, F_1 - \tilde{F}_U \rangle + \lambda^{-1} \left(-\frac{1}{2} + \frac{\lambda h}{4} \right) |w|^2 \\
&\quad + \lambda^{-1} E \left(\frac{\lambda^2 h^2}{4} + \frac{\lambda h}{4} \right) \lambda^{-1} E\langle w, F_1 - \tilde{F}_U \rangle + \lambda^{-1} \left(\frac{\lambda h}{2} + 2 \right) \lambda^{-1} E\langle w, F_2 - \tilde{F}_U \rangle \\
&\quad + \lambda^{-1} \left(\frac{\lambda^3 h^3}{16} \right) \lambda^{-2} E|F_1 - \tilde{F}_U|^2 + \lambda^{-1} (\lambda h) \lambda^{-2} E|F_2 - \tilde{F}_U|^2 \\
&\quad + \lambda^{-1} \left(\frac{\lambda^2 h^2}{4} \right) \lambda^{-2} E\langle F_1 - \tilde{F}_U, F_2 - \tilde{F}_U \rangle \\
&= \Gamma_0 + \Lambda_0 + \lambda^{-1} \frac{\lambda h}{4} E\langle z, \Delta F_1 \rangle + \lambda^{-1} \frac{1}{2} \langle z, E \Delta F_2 \rangle \\
&\quad + \lambda^{-1} \left(\frac{\lambda^2 h^2}{4} + \frac{\lambda h}{4} \right) E\langle w, \lambda^{-1} \Delta F_1 \rangle + \lambda^{-1} \left(\frac{\lambda h}{2} + 2 \right) \langle w, \lambda^{-1} E \Delta F_2 \rangle \\
&\quad + \lambda^{-1} \left(\frac{\lambda^3 h^3}{8} + \frac{\lambda^2 h^2}{4} \right) E\langle \lambda^{-1} \Delta F_1, \lambda^{-1} \Delta F_U \rangle \\
&\quad + \lambda^{-1} \left(\frac{\lambda^2 h^2}{4} + 2\lambda h \right) E\langle \lambda^{-1} \Delta F_2, \lambda^{-1} \Delta F_U \rangle \\
&\quad + \lambda^{-1} \left(\frac{\lambda^3 h^3}{16} \right) \lambda^{-2} E|\Delta F_1|^2 + \lambda^{-1} (\lambda h) \lambda^{-2} E|\Delta F_2|^2 \\
&\quad + \lambda^{-1} \left(\frac{\lambda^2 h^2}{4} \right) E\langle \lambda^{-1} \Delta F_1, \lambda^{-1} \Delta F_2 \rangle,
\end{aligned}$$

where Γ_0 and Λ_0 are the loss and gain from $\tilde{\mathcal{G}}^C \rho(y)^2$ in (74) and (75), respectively. Now we decompose $\mathcal{A}^C \rho(y)^2$

$$\mathcal{A}^C \rho(y)^2 \leq \Gamma + \Lambda + \Delta \quad \text{where} \quad \Gamma := \Gamma_0, \quad (82)$$

$$\Lambda := \Lambda_0 + \lambda^{-1} \frac{K}{18} |z|^2 + \lambda^{-1} \frac{1}{18} |w|^2 + \lambda^{-1} \left(\frac{\lambda^3 h^3}{16} + \frac{\lambda^2 h^2}{4} + \lambda h \right) \lambda^{-2} E|\Delta F_U|^2, \quad (83)$$

$$\begin{aligned}
\Delta &:= \lambda^{-1} \left(\frac{9}{4K\lambda^{-2}} + 36 \left(1 + \frac{\lambda h}{4} \right)^2 \right) \lambda^{-2} |E \Delta F_2|^2 \\
&\quad + \lambda^{-1} \left(\frac{\lambda^3 h^3}{8} + \frac{\lambda^2 h^2}{4} + \frac{9\lambda^2 h^2}{16K\lambda^{-2}} + 36 \left(\frac{\lambda^2 h^2}{8} + \frac{\lambda h}{8} \right)^2 \right) \lambda^{-2} E|\Delta F_1|^2 \\
&\quad + \lambda^{-1} \left(2\lambda h + \frac{\lambda^2 h^2}{4} \right) \lambda^{-2} E|\Delta F_2|^2. \quad (84)
\end{aligned}$$

Here the loss Λ in $\mathcal{A}^C \rho(y)^2$ was separated from the discretization error Δ by applying the Peter-Paul inequality to the four cross terms involving z or w (i.e.,

$E\langle z, \Delta F_1 \rangle$, $E\langle z, \Delta F_2 \rangle$, $E\langle w, \lambda^{-1} \Delta F_1 \rangle$, and $E\langle w, \lambda^{-1} \Delta F_2 \rangle$), and Young's product inequality for the remaining cross terms. As expected, the gain in (82) is the same as the gain in (74). We next bound the loss and discretization error terms separately.

For the loss Λ in (83), apply the Peter-Paul inequality with parameter $(L\lambda^{-2})^{1/2}$, $\lambda h \leq 1$, and (73), to obtain

$$\begin{aligned}
\Lambda &\leq \lambda^{-1} \frac{K}{18} |z|^2 + \lambda^{-1} \frac{1}{18} |w|^2 \\
&\quad + \lambda^{-1} \left(\frac{\lambda^3 h^3}{8} + \frac{\lambda^2 h^2}{2} + 2\lambda h + \frac{1}{2(L\lambda^{-2})^{1/2}} \left(\frac{\lambda^2 h^2}{4} + \frac{3\lambda h}{4} + 2 \right) \right) \lambda^{-2} E|\Delta F_U|^2 \\
&\quad + \lambda^{-1} \left(\frac{\lambda h}{4} + \frac{(L\lambda^{-2})^{1/2}}{2} \left(\frac{\lambda^2 h^2}{4} + \frac{3\lambda h}{4} + 2 \right) \right) |w|^2 \\
&\stackrel{(64)}{\leq} \lambda^{-1} \frac{K}{18} |z|^2 + \lambda^{-1} \frac{1}{18} |w|^2 \\
&\quad + \lambda^{-1} \left(\frac{21}{8} + \frac{3}{2(L\lambda^{-2})^{1/2}} \right) \lambda^{-2} E|\Delta F_U|^2 + \lambda^{-1} \left(\frac{1}{4} + \frac{3(L\lambda^{-2})^{1/2}}{2} \right) |w|^2 \\
&\stackrel{(73)}{\leq} \lambda^{-1} \frac{K}{18} |z|^2 + \lambda^{-1} \frac{1}{18} |w|^2 \\
&\quad - \lambda^{-1} \left(\frac{21L\lambda^{-2}}{8} + \frac{3(L\lambda^{-2})^{1/2}}{2} \right) E\langle Z_U, \Delta F_U \rangle + \lambda^{-1} \left(\frac{1}{4} + \frac{3(L\lambda^{-2})^{1/2}}{2} \right) |w|^2 \\
&\stackrel{(63)}{\leq} -\lambda^{-1} \left(\frac{21}{8 \cdot 12^2} + \frac{1}{8} \right) E\langle Z_U, \Delta F_U \rangle + \lambda^{-1} \frac{K}{18} |z|^2 + \lambda^{-1} \frac{31}{72} |w|^2. \tag{85}
\end{aligned}$$

Combining (82) with (85), and following the corresponding steps in the proof of Lemma 16, we obtain

$$\begin{aligned}
\Gamma + \Lambda &\leq \lambda^{-1} \left(\frac{137}{384} \right) E\langle Z_U, \Delta F_U \rangle + \lambda^{-1} \frac{K}{18} |z|^2 - \lambda^{-1} \frac{5}{72} |w|^2 \\
&\stackrel{(73)}{\leq} -\lambda^{-1} \left(\frac{137}{384} \right) KE|Z_U|^2 + \lambda^{-1} \frac{K}{18} |z|^2 - \lambda^{-1} \frac{5}{72} |w|^2 \\
&\leq -\lambda^{-1} \left(\frac{137}{384} \right) K(|z|^2 + h\langle z, w \rangle + \frac{h^2}{3} |w|^2) + \lambda^{-1} \frac{K}{18} |z|^2 - \lambda^{-1} \frac{5}{72} |w|^2 \\
&\leq -\lambda^{-1} \left(\frac{137}{384} \right) K \left(\frac{1}{2} |z|^2 + \left(\frac{h^2}{3} - \frac{h^2}{2} \right) |w|^2 \right) + \lambda^{-1} \frac{K}{18} |z|^2 - \lambda^{-1} \frac{5}{72} |w|^2 \\
&\stackrel{(63)}{\leq} -\frac{1}{16} \lambda^{-1} (K|z|^2 + |w|^2) \stackrel{(61)}{\leq} -\frac{1}{16} \lambda^{-1} \min\left(\frac{12}{13} \lambda^2, K\right) \rho(y)^2 \\
&\leq -\frac{1}{18} \min(\lambda, K\lambda^{-1}) \rho(y)^2. \tag{86}
\end{aligned}$$

Note that the numerical pre-factors appearing in the last few steps were simplified for readability.

For the discretization error Δ in (84), apply $\lambda h \leq 1$, and insert (80) and (81),

$$\begin{aligned}
\Delta &= \left(\frac{\lambda^2 h^2}{8} + \frac{\lambda h}{4} + 36\lambda h \left(\frac{\lambda h}{8} + \frac{1}{8} \right)^2 + \frac{9\lambda h}{16K\lambda^{-2}} \right) \lambda^{-2} h E |\Delta F_1|^2 \\
&\quad + \left(2 + \frac{\lambda h}{4} \right) \lambda^{-2} h E |\Delta F_2|^2 + \lambda^{-1} \left(36 \left(1 + \frac{\lambda h}{4} \right)^2 + \frac{9}{4K\lambda^{-2}} \right) \lambda^{-2} |E \Delta F_2|^2 \\
&\stackrel{(64)}{\leq} \left(\frac{21}{8} + \frac{9}{16K\lambda^{-2}} \right) \lambda^{-2} h E |\Delta F_1|^2 + \left(\frac{9}{4} \right) \lambda^{-2} h E |\Delta F_2|^2 \\
&\quad + \lambda^{-1} \left(\frac{225}{4} + \frac{9}{4K\lambda^{-2}} \right) \lambda^{-2} |E \Delta F_2|^2 \\
&\leq 11 \left(\frac{39}{8} + \frac{9}{16K\lambda^{-2}} \right) (L\lambda^{-2}) L h^3 (L^2 h^2 |x|^2 + |v|^2) \\
&\quad + \frac{1}{12} \left(\frac{225}{4} + \frac{9}{4K\lambda^{-2}} \right) (L\lambda^{-2})^{3/2} L^{3/2} h^4 (L|x|^2 + |v|^2) \\
&\stackrel{(63)}{\leq} \frac{1}{2} \left(1 + \frac{1}{K\lambda^{-2}} \right) L h^3 (L^{3/2} h |x|^2 + |v|^2) \tag{87}
\end{aligned}$$

where in the last step several of the numerical pre-factors were rounded up to unity for readability.

Combining (86) and (87) gives (68) — as required. \square

References

- [1] F. Achleitner, A. Arnold, and D. Stürzer. “Large-time behavior in non-symmetric Fokker-Planck equations”. In: *arXiv preprint arXiv:1506.02470* (2015) (cit. on pp. 9, 19, 25).
- [2] S. Blanes, F. Casas, and J. M. Sanz-Serna. “Numerical integrators for the Hybrid Monte Carlo method”. In: *SIAM Journal on Scientific Computing* 36.4 (2014), A1556–A1580 (cit. on p. 2).
- [3] N. Bou-Rabee and A. Eberle. *Markov Chain Monte Carlo Methods*. URL: <https://wt.iam.uni-bonn.de/eberle/>. Nov. 2020 (cit. on pp. 3, 7, 13).
- [4] N. Bou-Rabee and J. M. Sanz-Serna. “Geometric Integrators and the Hamiltonian Monte Carlo Method”. In: *Acta Numerica* 27 (2018), pp. 113–206 (cit. on pp. 2, 23).
- [5] N. Bou-Rabee and A. Eberle. “Mixing Time Guarantees for Unadjusted Hamiltonian Monte Carlo”. In: *Bernoulli* 29.1 (2023), pp. 75–104 (cit. on pp. 3, 9).
- [6] N. Bou-Rabee, A. Eberle, and R. Zimmer. “Coupling and convergence for Hamiltonian Monte Carlo”. In: *Ann. Appl. Probab.* 30.3 (2020), pp. 1209–1250 (cit. on pp. 2, 18).
- [7] N. Bou-Rabee and J. M. Sanz-Serna. “Randomized Hamiltonian Monte Carlo”. In: *Ann. Appl. Probab.* 27.4 (Aug. 2017), pp. 2159–2194. DOI: [10.1214/16-AAP1255](https://doi.org/10.1214/16-AAP1255). URL: <https://doi.org/10.1214/16-AAP1255> (cit. on pp. 5, 8, 23, 25).

- [8] N. Bou-Rabee and K. Schuh. “Convergence of Unadjusted Hamiltonian Monte Carlo for Mean-Field Models”. arXiv preprint arXiv:2009.08735. 2020 (cit. on pp. 2, 3, 10, 14–16).
- [9] E. Cancés, F. Legoll, and G. Stoltz. “Theoretical and Numerical Comparison of Some Sampling Methods for Molecular Dynamics”. In: *Mathematical Modelling and Numerical Analysis* 41 (2007), pp. 351–389 (cit. on p. 23).
- [10] Y. Cao, J. Lu, and L. Wang. “Complexity of randomized algorithms for underdamped Langevin dynamics”. In: *Communications in Mathematical Sciences* 19.7 (2021), pp. 1827–1853. DOI: [10.4310/cms.2021.v19.n7.a4](https://doi.org/10.4310/cms.2021.v19.n7.a4). URL: <https://doi.org/10.4310%2Fcms.2021.v19.n7.a4> (cit. on p. 4).
- [11] F. Casas, J. M. Sanz-Serna, and L. Shaw. “A New Optimality Property of Strang’s Splitting”. In: *arXiv preprint arXiv:2210.07048* (2022) (cit. on p. 2).
- [12] Y. Chen, R. Dwivedi, M. J. Wainwright, and B. Yu. “Fast mixing of Metropolized Hamiltonian Monte Carlo: Benefits of multi-step gradients”. In: *Journal of Machine Learning Research* 21.92 (2020), pp. 1–72 (cit. on pp. 2, 3, 9).
- [13] Z. Chen and S. S. Vempala. “Optimal convergence rate of Hamiltonian Monte Carlo for strongly logconcave distributions”. In: *Theory of Computing* 18.1 (2022), pp. 1–18. DOI: [10.4086/toc.2022.v018a009](https://doi.org/10.4086/toc.2022.v018a009). URL: <https://doi.org/10.4086/toc.2022.v018a009> (cit. on pp. 13, 16).
- [14] X. Cheng, N. S. Chatterji, P. L. Bartlett, and M. I. Jordan. “Underdamped Langevin MCMC: A non-asymptotic analysis”. In: *Conference On Learning Theory*. 2018, pp. 300–323 (cit. on p. 4).
- [15] X. Cheng, N. S. Chatterji, Y. Abbasi-Yadkori, P. L. Bartlett, and M. I. Jordan. “Sharp convergence rates for Langevin dynamics in the nonconvex setting”. In: *arXiv preprint arXiv:1805.01648* (2018) (cit. on p. 2).
- [16] A. S. Dalalyan and L. Riou-Durand. “On sampling from a log-concave density using kinetic Langevin diffusions”. In: *Bernoulli* 26.3 (2020), pp. 1956–1988 (cit. on p. 4).
- [17] T. Daun. “On the randomized solution of initial value problems”. In: *Journal of Complexity* 27.3 (2011). Dagstuhl 2009, pp. 300–311. ISSN: 0885-064X. DOI: <https://doi.org/10.1016/j.jco.2010.07.002>. URL: <https://www.sciencedirect.com/science/article/pii/S0885064X1000066X> (cit. on p. 4).
- [18] S. Duane, A. D. Kennedy, B. J. Pendleton, and D. Roweth. “Hybrid Monte-Carlo”. In: *Phys Lett B* 195 (1987), pp. 216–222 (cit. on p. 1).
- [19] A. Durmus and A. Eberle. “Asymptotic bias of inexact Markov Chain Monte Carlo Methods in High Dimension”. arXiv:2108.00682 [math.PR]. 2021 (cit. on pp. 10, 14, 15).
- [20] A. Durmus and E. Moulines. “High-dimensional Bayesian inference via the unadjusted Langevin algorithm”. In: *Bernoulli* 25.4A (2019), pp. 2854–2882 (cit. on p. 13).

- [21] Y. Fang, J. M. Sanz-Serna, and R. D. Skeel. “Compressible generalized hybrid Monte Carlo”. In: *Journal of chemical physics* 140.17 (2014), p. 174108 (cit. on p. 2).
- [22] J. Foster, T. Lyons, and H. Oberhauser. “The shifted ODE method for underdamped Langevin MCMC”. In: (2021). DOI: [10.48550/ARXIV.2101.03446](https://doi.org/10.48550/ARXIV.2101.03446). URL: <https://arxiv.org/abs/2101.03446> (cit. on p. 5).
- [23] Y. He, K. Balasubramanian, and M. A. Erdogdu. “On the Ergodicity, Bias and Asymptotic Normality of Randomized Midpoint Sampling Method”. In: *Advances in Neural Information Processing Systems*. Ed. by H. Larochelle, M. Ranzato, R. Hadsell, M. Balcan, and H. Lin. Vol. 33. Curran Associates, Inc., 2020, pp. 7366–7376. URL: <https://proceedings.neurips.cc/paper/2020/file/5265d33c184af566aeb7ef8afd0b9b03-Paper.pdf> (cit. on p. 4).
- [24] M. D. Hoffman and A. Gelman. “The no-U-turn sampler: Adaptively setting path lengths in Hamiltonian Monte Carlo”. In: *Journal of Machine Learning Research* 15.1 (2014), pp. 1593–1623 (cit. on p. 9).
- [25] M. D. Hoffman and P. Sountsov. “Tuning-Free Generalized Hamiltonian Monte Carlo”. In: *International Conference on Artificial Intelligence and Statistics*. PMLR, 2022, pp. 7799–7813 (cit. on p. 9).
- [26] B. Kacewicz. “Almost Optimal Solution of Initial-Value Problems by Randomized and Quantum Algorithms”. In: (2005). DOI: [10.48550/ARXIV.QUANT-PH/0510045](https://doi.org/10.48550/ARXIV.QUANT-PH/0510045). URL: <https://arxiv.org/abs/quant-ph/0510045> (cit. on p. 4).
- [27] B. Kacewicz. “Randomized and quantum algorithms yield a speed-up for initial-value problems”. In: *Journal of Complexity* 20.6 (2004), pp. 821–834. ISSN: 0885-064X. DOI: <https://doi.org/10.1016/j.jco.2004.05.002>. URL: <https://www.sciencedirect.com/science/article/pii/S0885064X04000317> (cit. on p. 4).
- [28] T. S. Kleppe. “Connecting the Dots: Numerical Randomized Hamiltonian Monte Carlo with State-Dependent Event Rates”. In: *Journal of Computational and Graphical Statistics* 31.4 (2022), pp. 1238–1253. DOI: [10.1080/10618600.2022.2066679](https://doi.org/10.1080/10618600.2022.2066679). eprint: <https://doi.org/10.1080/10618600.2022.2066679>. URL: <https://doi.org/10.1080/10618600.2022.2066679> (cit. on p. 9).
- [29] Y. T. Lee, Z. Song, and S. S. Vempala. “Algorithmic theory of ODEs and sampling from well-conditioned logconcave densities”. In: *arXiv preprint arXiv:1812.06243* (2018) (cit. on p. 2).
- [30] P. B. Mackenzie. “An improved hybrid Monte Carlo method”. In: *Physics Letters B* 226.3 (1989), pp. 369–371 (cit. on p. 23).
- [31] O. Mangoubi and A. Smith. “Mixing of Hamiltonian Monte Carlo on strongly log-concave distributions: Continuous Dynamics”. In: *Ann. Appl. Probab.* 31.5 (2021), pp. 2019–2045 (cit. on p. 13).
- [32] J. C. Mattingly, A. M. Stuart, and D. J. Higham. “Ergodicity for SDEs and approximations: locally Lipschitz vector fields and degenerate noise”. In: *Stoch. Proc. Appl.* 101.2 (2002), pp. 185–232 (cit. on pp. 5, 25).

- [33] J. C. Mattingly, A. M. Stuart, and M. V. Tretyakov. “Convergence of numerical time-averaging and stationary measures via Poisson equations”. In: *SIAM J Num Anal* 48.2 (2010), pp. 552–577 (cit. on p. 15).
- [34] G. N. Milstein and M. V. Tretyakov. “Mean-Square Approximation for Stochastic Differential Equations”. In: *Stochastic Numerics for Mathematical Physics*. Cham: Springer International Publishing, 2021, pp. 1–94 (cit. on pp. 7, 14).
- [35] P. Monmarché. “HMC and underdamped Langevin united in the unadjusted convex smooth case”. In: (2022). DOI: [10.48550/ARXIV.2202.00977](https://doi.org/10.48550/ARXIV.2202.00977). URL: <https://arxiv.org/abs/2202.00977> (cit. on pp. 2, 4, 8).
- [36] R. M. Neal. “MCMC using Hamiltonian dynamics”. In: *Handbook of Markov Chain Monte Carlo 2* (2011), pp. 113–162 (cit. on pp. 1, 23).
- [37] G. Quispel and D. I. McLaren. “A new class of energy-preserving numerical integration methods”. In: *Journal of Physics A: Mathematical and Theoretical* 41.4 (2008), p. 045206 (cit. on p. 7).
- [38] J. M. Sanz-Serna and A. M. Stuart. “Ergodicity of dissipative differential equations subject to random impulses”. In: *Journal of Differential Equations* 155.2 (1999), pp. 262–284 (cit. on p. 25).
- [39] R. Shen and Y. T. Lee. “The randomized midpoint method for log-concave sampling”. In: *Advances in Neural Information Processing Systems* 32 (2019) (cit. on pp. 2, 4).
- [40] D. Talay. “Stochastic Hamiltonian Systems: Exponential Convergence to the Invariant Measure, and Discretization by the Implicit Euler Scheme”. In: *Markov Processes and Related Fields* 8 (2002), pp. 1–36 (cit. on p. 25).

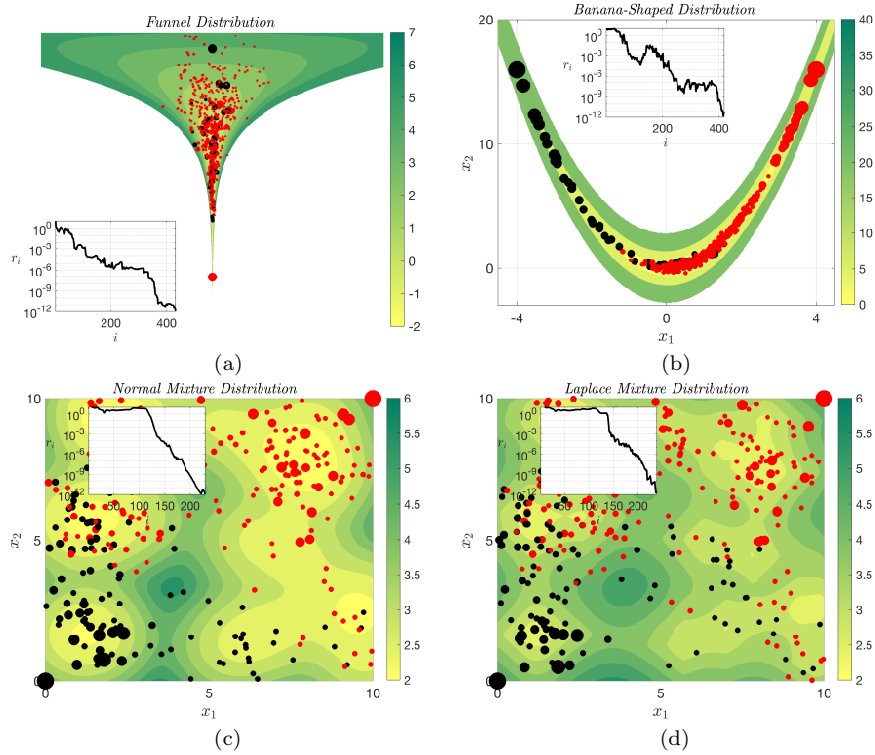


FIG 1. Realizations of Synchronous Coupling. Although we only prove contractivity of a synchronous coupling for strongly convex and gradient Lipschitz U in Theorem 6, the synchronous coupling appears to contract in a variety of non-convex models. In particular, this figure illustrates realizations of a synchronous coupling with duration $T = 1$, time step sizes $h = 0.01$ in (a)-(b) and $h = 0.1$ in (c)-(d), for the indicated target distributions. The different components of the coupling are shown as different color dots. The size of the dots is related to the number of steps: points along the trajectory corresponding to a larger number of steps have smaller markers. A contour plot of the underlying potential energy function is shown in the background. The inset plots the distance r_i between the components of the coupling as a function of the uHMC step index i . The simulation is terminated when this distance first reaches 10^{-12} . In (a), (b), (c), and (d), this occurs in 433, 420, 231 and 239 steps, respectively.

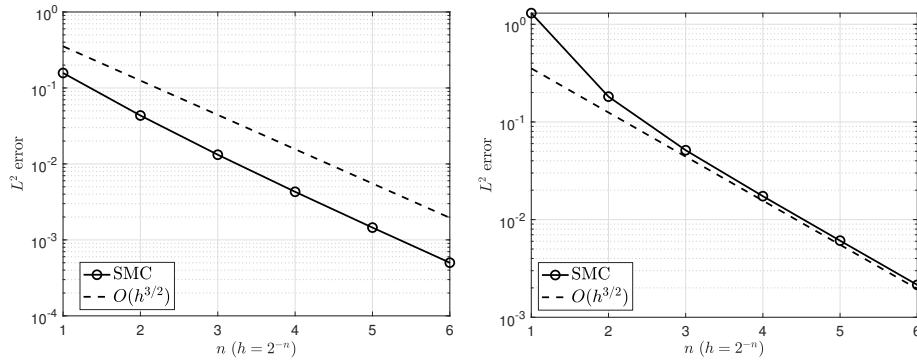


FIG 2. **L^2 -Accuracy Verification.** *Left Image:* A plot of the L^2 -error in (x, v) -space of the sMC time integrator for the linear oscillator with Hamiltonian $H(x, v) = (1/2)(v^2 + x^2)$. *Right Image:* A plot of the L^2 -error in (x, v) -space of the sMC time integrator for a double-well system with Hamiltonian $H(x, v) = (1/2)(v^2 + (1 - x^2)^2)$. Both simulations have initial condition $(2, 1)$ and unit duration. The time step sizes tested are 2^{-n} where n is given on the horizontal axis. The dashed curve is $2^{-3n/2} = h^{3/2}$ versus n .